The wave energy flux of high frequency diffracting beams in complex geometrical optics

Omar Maj, Alberto Mariani, Emanuele Poli, and Daniela Farina

Citation: Physics of Plasmas (1994-present) **20**, 042122 (2013); doi: 10.1063/1.4802935
View online: http://dx.doi.org/10.1063/1.4802935
View Table of Contents: http://scitation.aip.org/content/aip/journal/pop/20/4?ver=pdfcov
Published by the AIP Publishing

The wave energy flux of high frequency diffracting beams in complex geometrical optics

Omar Maj,[1,a)] Alberto Mariani,[2,3] Emanuele Poli,[1] and Daniela Farina[2]
[1]*Max Planck Institute for Plasma Physics, EURATOM Association, Boltzmannstr. 2, 85748 Garching, Germany*
[2]*Istituto di Fisica del Plasma "P. Caldirola," Consiglio Nazionale delle Ricerche, EURATOM-ENEA-CNR Association, via R. Cozzi 53, I-20125 Milano, Italy*
[3]*Università degli Studi di Milano, Dipartimento di Fisica, Via Celoria 16, 20133 Milano, Italy*

(Received 28 November 2012; accepted 11 April 2013; published online 30 April 2013)

We consider the construction of asymptotic solutions of Maxwell's equations for a diffracting wave beam in the high frequency limit and address the description of the wave energy flux transported by the beam. With this aim, the complex eikonal method is applied. That is a generalization of the standard geometrical optics method in which the phase function is assumed to be complex valued, with the non-negative imaginary part accounting for the finite width of the beam cross section. In this framework, we propose an argument which simplifies significantly the analysis of the transport equation for the wave field amplitude and allows us to derive the wave energy flux. The theoretical analysis is illustrated numerically for the case of electron cyclotron beams in tokamak plasmas by using the GRAY code [D. Farina, Fusion Sci. Technol. **52**, 154 (2007)], which is based upon the complex eikonal theory. The results are compared to those of the paraxial beam tracing code TORBEAM [E. Poli *et al*., Comput. Phys. Commun. **136**, 90 (2001)], which provides an independent calculation of the energy flow. [http://dx.doi.org/10.1063/1.4802935]

I. INTRODUCTION

The description of high-frequency beams in inhomogeneous dispersive media is usually dealt with by means of asymptotic methods that greatly simplify the computational problem. This is the case of electron cyclotron heating and current drive applications in large magnetic confinement devices, where the wave-length to plasma-size ratio is extremely small, thus hampering the direct numerical solution of the relevant wave equation. One such method is complex geometrical optics. Specifically, the version of the complex geometrical optics method implemented in the GRAY code[1] has gained interest in the last few years, and, together with the beam tracing code TORBEAM,[2] constitutes a major tool for the design of electron cyclotron heating and current drive systems.[3]

The term "complex geometrical optics," rather than to a unified theory, refers to a family of closely related methods for the construction of a uniform asymptotic solution of wave equations in the high-frequency limit capturing wave effects such as diffraction. It is a development of high-frequency diffraction theory,[4] and as such it builds on and extends the standard geometrical optics method. (Among the vast literature available on standard geometrical optics, one can refer to the monograph by Kravtsov and Orlov[5] for a physics overview, to the review paper by McDonald[6] for more insights on operators and symbol calculus, and to Rauch's lectures[7] for mathematically rigorous results with emphasis on symmetric hyperbolic systems.)

In addition to the variety of complex geometrical optics flavors, other methods such as the paraxial WKB method developed by Pereverzev,[8,9] the complex WKB method,[10] and the theory of Gaussian beams[11–13] are deeply related to the techniques and ideas of complex geometrical optics.[14–16]

An attempt to a systematic classification of such various aspects of complex geometrical optics has been made in the recent monograph by Kravtsov,[17] which includes a comprehensive list of references and a brief historical account; cf. also Červený[18] and references therein. Concerning plasma physics applications, one might distinguish two main branches.

The first branch is complex ray theory, also known as ray-based complex geometrical optics, which relies on the complexification of standard geometrical optics rays (cf. the review papers by Kravtsov *et al*.,[19] Thomson,[20] and Chapman *et al*.,[21] as well as the numerical implementations of Egorchenkov and Kravtsov[22] and Amodei *et al*.[23] and references therein). This has been applied to plasma physics for the description of strong damping,[24–26] although complex rays can be used to describe diffractive beams as well.[19,21]

The second branch is the complex eikonal theory,[27] also known as eikonal-based complex geometrical optics, which has been applied to fusion-relevant problems by Mazzucato,[28] Nowak and Orefice,[29–31] Peeters,[32] Timofeev,[33] and which eventually led to the GRAY code.[1] Instead of relying on the complexification of geometrical optics rays, a new set of trajectories in the real space, called extended rays,[32] are defined as a perturbation of standard geometrical optics rays due to diffraction.

Both forms of the complex geometrical optics share the same ansatz for the wave field, which is built upon the standard WKB ansatz of geometrical optics by replacing the real-valued eikonal with a complex-valued function referred to as complex eikonal.

a)Electronic mail: omaj@ipp.mpg.de

The imaginary part of the complex eikonal should be non-negative to avoid a blow-up of the field in the high frequency limit. It was recognized by Pereverzev[9] and Maslov[10] that the non-negative imaginary part of the eikonal implies a localization of the wave field.

In this work, we propose a modified argument for the derivation of the complex geometrical optics equations, i.e., the partial differential equations for the complex eikonal and the amplitude of the wave field. Besides providing a better mathematical foundation to the method, this argument allows us to obtain the wave energy flux straightforwardly from the amplitude transport equation. Our approach consists in exploiting the localization of the wave field in order to obtain a sharper control of the order of terms in the high frequency asymptotic expansion of the wave equation, as done by Pereverzev and Maslov in different contexts.

The theory is then illustrated numerically by means of the GRAY[1] and TORBEAM[2] codes for the case of electron cyclotron beams in tokamak plasmas. In particular, a comparison between the energy flows computed by GRAY and TORBEAM is reported.

In those simulations, extended rays are computed with the standard GRAY code, which has been equipped with new diagnostics. As for the beam tracing code TORBEAM, the wave energy flow is computed by a module, which has been recently added[34] as an interface of the code with ray-based quasi-linear Fokker-Planck solvers.

At last, a generalization of the theory to dispersive, weakly dissipative media is sketched, showing in particular the robustness of high-frequency wave asymptotics. Possible applications encompass electrodynamics, elastodynamics, linear waves in fluids and plasmas, as well as quantum mechanics in the semiclassical limit. Our main concern however is heating and current drive mechanisms in tokamak plasmas. Therefore, all numerical results refer to electron cyclotron wave beams in tokamak geometry, for which a standard ITER plasma equilibrium is used.

The paper is organized as follows. In Sec. II, we review the basic results of the standard geometrical optics, and introduce the complex eikonal theory in its standard derivation. This review material is not new, but it helps us to keep the paper self-contained, defines the notation, and explains basic ideas in a simple context. The standard approach to the complex eikonal theory is critically outlined in Sec. II B, explaining in particular the main motivations for this work. The estimates of Pereverzev and Maslov, which constitute the fundamental tool employed here, are also reviewed and adapted to our framework in Sec. II C. Section III is devoted to the derivation of complex geometrical optics equations and the wave energy flux, while Sec. IV reports numerical results. The results of Sec. III are derived for the simple case of spatially non-dispersive media, i.e., when the response of the medium to the electromagnetic perturbation is local, and thus Maxwell's equations for the electromagnetic fields in the medium amount to partial differential equations. In the general case of spatially dispersive media, however, the response of the medium is non-local. Then, Maxwell's equations involve pseudodifferential operators.[6] In Sec. V, we show how the theory can be extended to the case of spatially dispersive media.

II. REVIEW OF STANDARD AND COMPLEX GEOMETRICAL OPTICS

In this section, we fix the notation and review basic results and ideas, upon which the complex geometrical optics method relies.

For sake of simplicity, we consider here spatially non-dispersive media for which the constitutive relation between the electric displacement D and the electric field E is local, namely, $D = \varepsilon E$ where ε is a matrix referred to as the dielectric tensor. In Sec. V, we describe the modifications of the theory required for the case of spatially dispersive media, i.e., when ε is replaced by a pseudodifferential operator.

A. The wave equation and standard geometrical optics

Let us start from the equation for the electric field of a monochromatic electromagnetic wave beam in a stationary spatially non-dispersive medium, namely,

$$\nabla \times (\nabla \times E(\kappa, x)) - \kappa^2 \varepsilon(\kappa, x) E(\kappa, x) = 0. \tag{1}$$

Equation (1) is written in the dimensionless form adopted by Pereverzev,[9] where the coordinates $x = (x^i)$, $i = 1, 2, 3$, are normalized to the scale L of typical spatial variations of the medium, and the large parameter

$$\kappa = \omega L / c$$

appears naturally. In addition, $\nabla = (\partial / \partial x^i)_i$ and c is the speed of light in free space. The dependence of the solution $E(\kappa, x)$ on the parameter κ is explicitly indicated, whereas the additional dependence on the beam frequency ω is implied in both the electric field E and the dielectric tensor ε of the medium.

We are interested in asymptotic solutions of (1) in the limit $\kappa \to +\infty$, which can be constructed by modest computational means, and yet provide excellent approximations of the exact wave field for many applications as far as the parameter κ is large. Asymptotic solutions offer an effective alternative to the major computational problem of direct numerical integration of (1) for very high frequencies in large three-dimensional domains.

As usual,[6,9] the dielectric tensor is assumed to be smooth and have the asymptotic expansion,

$$\varepsilon(\kappa, x) = \varepsilon_0(x) + \kappa^{-1} \varepsilon_1(x) + O(\kappa^{-2}), \tag{2}$$

in the limit $\kappa \to +\infty$, with ε_0 being Hermitian, i.e., $\varepsilon_0 = \varepsilon_0^*$. Therefore, the medium is weakly dissipative since the wave energy absorption coefficient[35] is related to the anti-Hermitian part $\varepsilon^a = \kappa^{-1} \varepsilon_1^a + O(\kappa^{-2})$, and this is vanishingly small as $\kappa \to +\infty$. (Here and throughout the paper, $A^h = (A + A^*)/2$ and $A^a = -i(A - A^*)/2$ denote the Hermitian and anti-Hermitian part of a matrix A, respectively, with A^* being the Hermitian conjugation, i.e., the transpose of the complex-conjugate of A.)

Upon testing the wave operator, i.e., the left-hand side of Eq. (1), with a plane wave $e^{i\kappa N \cdot x}$ and separating the

leading order in κ, one obtains the matrix-valued smooth function

$$\mathsf{D}_{0,ij}(x,N) = N^2\delta_{ij} - N_iN_j - \varepsilon_{0,ij}(x), \tag{3}$$

which is referred to as the dispersion tensor of the medium,[6,36] or, mathematically, as the semiclassical principal symbol[37] of the operator (1). This is defined on a domain in the x-N space, which is referred to as the wave phase space. In view of the definition of κ and the normalization of spatial coordinates x, the conjugate variable $N = (N_i)_i$ has the physical meaning of the refractive index vector.

In Sec. V, it will be shown that the dispersion tensor (3) can be naturally generalized to the case of spatially dispersive media. All subsequent results in this section remain valid provided that $\varepsilon(\kappa,x)$ is replaced by $\varepsilon(\kappa,x,N)$ defined in Sec. V.

The real eigenvalues λ_j of D_0 give the local dispersion functions of wave modes supported by the medium.[6] It is customary to assume that the eigenvalues λ_j are well separated, namely, there exists a strictly positive constant $C > 0$ such that $|\lambda_i(x,N) - \lambda_j(x,N)| \geq C$ for $i \neq j$ and for (x,N) in the relevant domain in the wave phase-space.[7] This implies that the dispersion surface of one mode does not get close to that of the other modes, and linear mode conversion is excluded,[6,7] that is, no energy exchange can take place among different modes. Hence under such hypothesis, each mode is independent of the others and Maxwell's Eq. (1) in the limit $\kappa \to +\infty$ can be reduced to decoupled scalar equations describing the various modes.[38] The much more difficult case of linear mode conversion[39–42] is beyond the scope of this paper.

Let us denote by $H(x,N)$ the eigenvalue of $\mathsf{D}_0(x,N)$ relevant to the considered mode, and let $e(x,N)$ be the corresponding unit eigenvector. For simplicity, we consider the case of simple eigenvalues, i.e., the corresponding eigenspace is assumed to be one-dimensional. The general case can be dealt with by using spectral projectors.[7,43]

In geometrical optics, a solution of Eq. (1) is sought in the form (eikonal ansatz)

$$E(\kappa,x) = e^{i\kappa S(x)}a(\kappa,x), \quad a(\kappa,x) \sim \sum_{j=0}^{+\infty} \kappa^{-j}a_j(x), \tag{4}$$

where $S(x)$ is a real-valued smooth function representing the short-scale oscillations of the field and referred to as the eikonal, while $a_j(x)$ are vector-valued complex smooth functions that will be generically referred to as amplitudes. The asymptotic sum $a(\kappa,x)$ of amplitudes is defined in the standard way.[37]

Upon substituting (4) into (1) and performing the asymptotic expansion in the limit $\kappa \to +\infty$, one finds that multiple solutions exist, one for each propagation mode supported by the medium. Under the conditions stated above, each mode is independent. We consider the one which corresponds to the eigenvalue-eigenvector pair $H(x,N)$, $e(x,N)$. Then, $a_0(x) = A(x)e(x,\nabla S(x))$, where $A(x)$ is a scalar complex amplitude, and the polarization of the leading order term in the geometrical optics solution is determined by the eigenvalue $e(x,N)$ for $N = \nabla S$.

The eikonal $S(x)$ is determined by the standard eikonal equation

$$H(x,\nabla S(x)) = 0. \tag{5a}$$

Given $S(x)$, the scalar amplitude $A(x)$ is determined by the amplitude transport equation

$$V(x)\cdot\nabla A(x) = [-\gamma_1(x) + i\delta_1(x) - \frac{1}{2}\nabla\cdot V(x)]A(x), \tag{5b}$$

where the vector field

$$V(x) = \partial H(x,\nabla S(x))/\partial N \tag{6}$$

plays the role of the group velocity,

$$\gamma_1 = e^*\cdot\varepsilon_1^a e, \tag{7}$$

accounts for wave damping, and

$$\delta_1 = e^*\cdot\varepsilon_1^h e + ie^*\cdot\{H,e\} - \frac{i}{2}\sum_{i,j}\mathsf{D}_{0,ij}\{e_i^*,e_j\}, \tag{8}$$

accounts for a lower order shift in the phase, due to the residual Hermitian part ε_1^h (usually zero) plus the effects of polarization transport extensively discussed by Littlejohn and Flynn[38] and Emmrich and Weinstein.[43] In both Eqs. (7) and (8), all phase space functions are evaluated at $N = \nabla S(x)$, e_i are the components of e, and Poisson brackets are defined by

$$\{f,g\} = \frac{\partial f}{\partial N_i}\frac{\partial g}{\partial x^i} - \frac{\partial f}{\partial x^i}\frac{\partial g}{\partial N_i}$$

with the reversed sign with respect to, e.g., Littlejohn and Flynn.[38] The usual convention for the sum over repeated up- and down-placed indices is adopted throughout the paper.

Equations (5) are referred to as geometrical optics equations. We do not digress here on the details of the derivation as this can be inferred by specializing the complex eikonal theory described in Sec. III. A direct derivation can be found in the report by McDonald,[6] while Kaufman *et al.*[44] proposed a variational derivation for the symmetric case ($\varepsilon_1 = 0$), identifying the Poisson-bracket structure of the phase-shift (8), cf. also Littlejohn and Flynn.[38] A general and compact derivation with emphasis on geometric structures is given by Emmrich and Weinstein.[43] (These references provide a general and modern view to the subject. We do not attempt here to give a complete historical account of the vast literature on the development of geometrical optics.)

The geometrical optics estimate of the residual can now be stated: given a (sufficiently regular) *classical* solution $S(x)$ and $A(x)$ of Eqs. (5) in a bounded domain, and setting $a_0(x) = A(x)e(x,\nabla S(x))$, there exists a corrector $a_1(x)$, such that the geometrical optics solution,

$$E_{\mathrm{GO}}(\kappa,x) = e^{i\kappa S(x)}(a_0(x) + \kappa^{-1}a_1(x)), \tag{9}$$

solves (1) with a residual

$$|\kappa^{-2}\nabla\times\nabla\times E_{\mathrm{GO}}(\kappa,x) - \varepsilon(\kappa,x)E_{\mathrm{GO}}(\kappa,x)| \leq C\kappa^{-2}, \tag{10}$$

uniformly for x in the considered domain, $C > 0$ being a constant. The leading order term in (1) is $O(\kappa^2)$, hence the whole equation has been multiplied by κ^{-2}. The error estimate (10) just controls the residual in the wave equation, but it does not say anything about the convergence of the geometrical optics solution to the exact solution. That would require a finer analysis.[7] The corrector $a_1(x)$ however is never evaluated in practice.

The actual construction of the geometrical optics field (9) requires the solution of geometrical optics Eqs. (5). Summarizing, the linear vector Eq. (1) has been reduced to the scalar nonlinear Eq. (5a) complemented by the scalar linear transport Eq. (5b). The nonlinearity of Eq. (5a) in particular might seem a disadvantage hardly compensated by the reduction to a scalar problem. One should notice however that geometrical optics Eqs. (5) are independent of κ, that is, the geometrical optics approximation allows us to remove the short scale length of the wave field oscillations from the problem. The nonlinearity is the price one has to pay for such a tremendous simplification. As a result, a direct numerical solution of (5) is viable and appropriate numerical methods have been developed in the framework of Eulerian geometrical optics, cf. the review papers by Benamou,[45] the method by Benamou *et al.*,[46,47] and the review by Runborg.[48]

In most applications, however the direct numerical solution of geometrical optics Eqs. (5) is usually not favored. The ray tracing technique is used instead, being simpler to implement and computationally faster. This relies on the fact that Eq. (5a) is a first-order nonlinear partial differential equation, for which the theory of characteristics applies, cf. chapter 1 Sec. 15 of Taylor's treatise.[49] Specifically, there is a deep connection between (5a) and the Hamiltonian system

$$\frac{dx^i}{d\tau} = \frac{\partial H}{\partial N_i}(x,N), \quad \frac{dN_i}{d\tau} = -\frac{\partial H}{\partial x^i}(x,N), \tag{11}$$

where the parameter τ plays the role of time. A solution $(x(\tau),N(\tau))$ satisfying the local dispersion relation $H(x,N)=0$ is referred to as a bi-characteristic curve of Eq. (5a), while its projection $x(\tau)$ into the physical space is called a geometrical optics ray.

The construction of a solution of (5a) using rays is obtained as follows. Let us assume, as boundary conditions, that the wave field is prescribed in the form $E_0(\kappa,y) \propto e^{i\kappa S_0(y)}$ on a $(d-1)$-dimensional smooth surface

$$\Sigma_0 = \{x;\ x = x_0(y)\},$$

parametrized by the variables $y=(y^i)$, $i=1,\ldots,d-1$, where $d \geq 2$ is the effective dimensionality of the problem (typically, $d=2$ or $d=3$). One can think of Σ_0 as the surface of either a mirror or an antenna, where the launched wave field is known.

The gradient of the initial phase $S_0(y)$, together with the local dispersion relation $H(x_0(y),N_0(y))=0$, yields the initial conditions $(x_0(y),N_0(y))$ for Hamilton's Eqs. (11). Specifically, $\nabla_y S_0$ determines the component of $N_0(y)$ tangent to Σ_0 at the point $x_0(y)$. Meaningful data must be such that the lifted surface,

$$\Lambda_0 = \{(x,N);\quad x = x_0(y),\quad N = N_0(y)\}, \tag{12}$$

is non-characteristic,[49] i.e., the Hamiltonian orbits of the system (11) originating from points of Λ_0 are transversal (not necessarily orthogonal) to Λ_0 itself, so that orbits move away from the surface, and $\nabla_N H_{|\Lambda_0} \neq 0$. Then, the solution of Hamilton's Eqs. (11) can be readily found in the form $(x(\tau,y),N(\tau,y))$ depending on the initial point y on the launching surface Σ_0. This defines a d-dimensional surface

$$\Lambda = \{(x,N);\quad x = x(\tau,y),\quad N = N(\tau,y)\}, \tag{13}$$

immersed into the $2d$-dimensional wave phase space, and parametrized by coordinates (τ,y). Indeed, Λ is the flow out of Λ_0 by the Hamiltonian flow.

As a consequence of the non-characteristic hypothesis on Λ_0, the relationship $x = x(\tau,y)$ defines a change of coordinates, at least locally near Σ_0. In analogy with fluid dynamics, the new coordinates (τ,y) are referred to as Lagrangian coordinates and the ray tracing technique is also referred to as Lagrangian geometrical optics,[45] as opposed to Eulerian geometrical optics. Geometrically, Lagrangian coordinates establish a one-to-one correspondence between a neighborhood of Σ_0 in the physical space and a neighborhood of Λ_0 in the surface Λ. By exploiting the geometrical properties of Λ (specifically Λ is a Lagrangian manifold[49–53]), it is possible to proof[49] that, at least near Σ_0, there exists a real function $S(x)$ such that $N(\tau,y) = \nabla S(x(\tau,y))$ and $S_{|\Sigma_0} = S_0(y)$. It follows that $S(x)$ solves Eq. (5a) with the appropriate boundary condition. Despite its rather abstract definition, the construction of S in Lagrangian coordinates is actually straightforward and can be combined with the construction of the corresponding amplitude A. Specifically, one has

$$\frac{\partial S}{\partial \tau} = N \cdot \frac{\partial H}{\partial N},$$
$$\frac{\partial A}{\partial \tau} = \left[-\gamma_1 + i\delta_1 - \frac{1}{2}\nabla \cdot V\right]A,$$

and this is a system of ordinary differential equations that can be conveniently integrated together with Hamilton's Eq. (11) by standard numerical techniques.

This construction however relies on the one-to-one correspondence between physical space and the Lagrangian manifold Λ, and this can be established locally only. Away from the surface Σ_0 geometrical optics rays can cross each other. Correspondingly, Λ turns vertical and fold onto itself so that, over a given point x in the physical space, multiple branches of Λ can exist. At such points, the value of $S(x)$ and $A(x)$ is not uniquely defined.

Figure 1 shows the surface Λ for simple cases in two dimensions ($d=2$). The phase space is four-dimensional, and yet one can obtain an effective visualization of Λ by exploiting the local dispersion relation to eliminate one dimension. This visualization concept has been recently suggested by Tracy *et al.*[54] Here, the simple case of transverse electromagnetic waves in an isotropic medium has been considered, for which the local dispersion relation reads[5]

$$H(x,N) = N^2 - n^2(x) = 0, \tag{14}$$

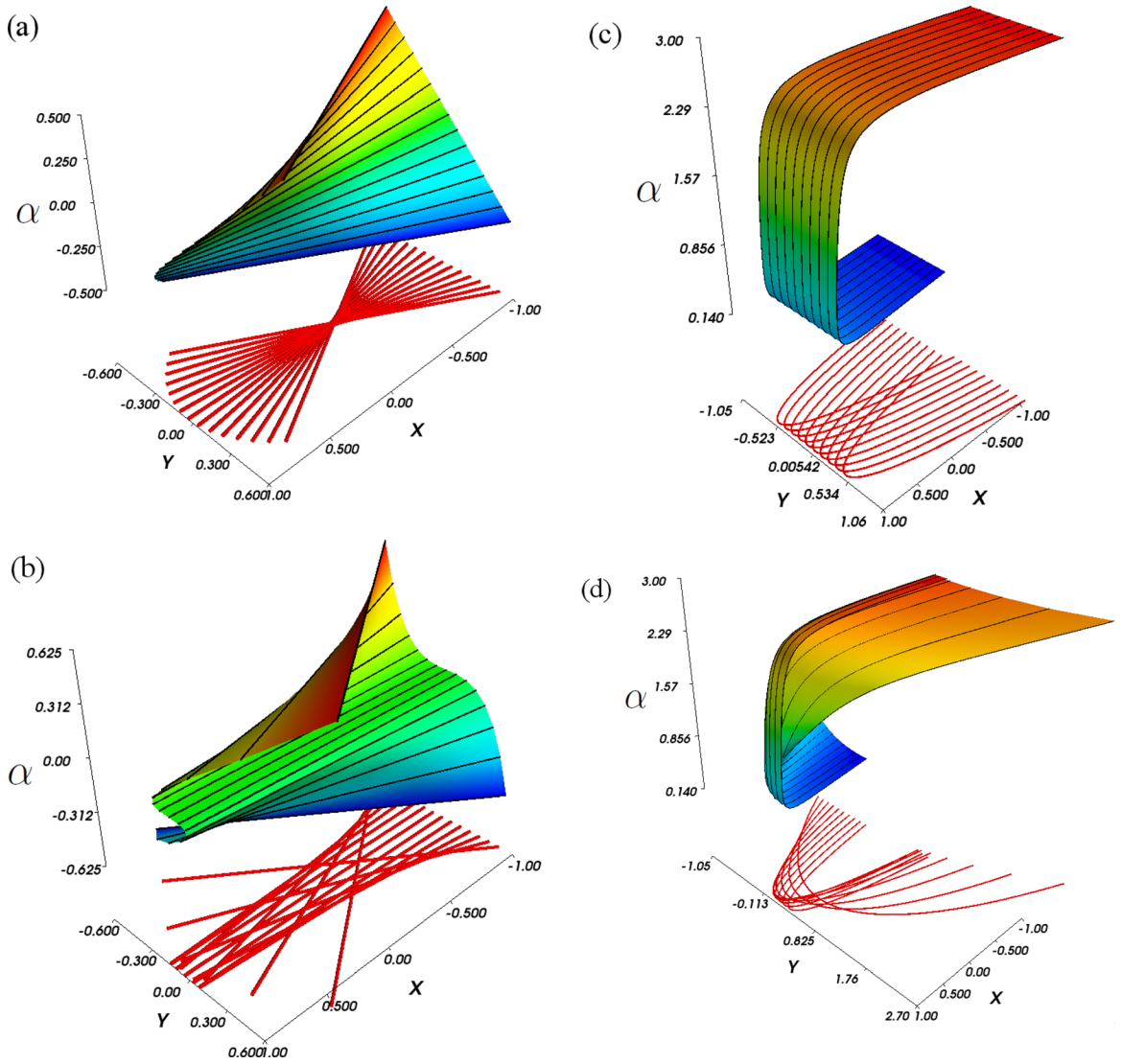

FIG. 1. Visualization of Lagrangian manifolds for two-dimensional models of wave propagation corresponding to the local dispersion relation (14): parabolic focal point in free space (a), quartic focal point in free-space (b), a fold caustic (c), and a fold combined with a focal point (d). The curves in the x-y plane represent selected rays, while the curves on the Lagrangian surface represent the corresponding Hamiltonian orbits in the phase space. The third axis is the angle α defined by $(N_x, N_y) = n(x, y)(\cos\alpha, \sin\alpha)$, which parametrizes the dispersion surface.

$n(x)$ being the refractive index. In two dimensions, let us write $x = (x^1, x^2) = (x, y)$ and $N = (N_1, N_2) = (N_x, N_y)$. Then, the dispersion manifold can be parametrized by (x, y, α), with $N_x = n(x, y)\cos\alpha$ and $N_y = n(x, y)\sin\alpha$, and the angle α is used as a third axis in Figure 1. The initial surface is $\Sigma_0 = \{(x, y);\ x = -1\}$, and the beam is launched toward the positive x-axis. The case of free space $n(x, y) = 1$ is shown in plots (a) and (b), for two different boundary conditions generating cusped singularities: parabolic launching mirror, $\alpha_{|\Sigma_0} = y$, (a) and a quartic launching mirror, $\alpha_{|\Sigma_0} = -5y^3$, (b). In the latter case, the Lagrangian surface Λ exhibits a rather complicated structure even in free space. Plots (c) and (d) show the classical model of reflection from a linear medium, for which $n^2(x, y) = (1 - x)/2$ with a cutoff at $x = 1$, where the refractive index vanishes. In the case of a plane wave (c) with an angle $\alpha_{|\Sigma_0} = \alpha_0 = 0.14$ ($\approx 8^\circ$), the Lagrangian manifold has a simple fold. For a focused beam (d) with $\alpha_{|\Sigma_0} = \alpha_0 - 0.3y^3$, a fold and a cusp are found together.

In all cases of Figure 1, the surface Λ cannot be projected one-to-one on the configuration space. Particularly, one can note that there are points $x = (x, y)$ above which Λ can be separated into a finite number branches, that merge in points where Λ turns vertical in the phase space. Those are the singular points of Λ, and their projection onto the configuration space defines the set of caustics.

Caustics pose an obstruction to the existence of classical solutions of the Hamilton-Jacobi Eq. (5a) for the phase. On caustics, the wave field amplitude blows up, with consequent loss of uniform approximation. In order to see this, let us consider the Jacobian matrix $U(\tau, y)$ of the map $(\tau, y) \mapsto x(\tau, y)$. Since $x(\tau, y)$ solves an ordinary differential equation, one can check that, in components,

$$\partial U^i_j / \partial \tau = (\nabla V)^i_k U^k_j,$$

and for the determinant $|U| = \det U$,

$$\partial|U|/\partial\tau = (\nabla \cdot V)|U|.$$

These are well known properties of ordinary differential equations, cf. the first chapter of Hörmander's lectures.[55] Equation (5b) in Lagrangian coordinates reads[5]

$$\begin{cases} A = |U|^{-\frac{1}{2}}\tilde{A}, \\ \partial\tilde{A}/\partial\tau = [-\gamma_1 + i\delta_1]\tilde{A}, \end{cases}$$

and the coefficients of the equation for $\tilde{A}$ are smooth on the whole wave phase space. Therefore, the equation for $\tilde{A}(\tau, y)$ can always be solved by a simple integration along the rays, and the result accounts for the amplitude damping and phase shift. The total amplitude A, on the other hand, depends on the Jacobian determinant $|U|$, which accounts for the convergence/divergence of the bundle of rays, that is, for the deformation of the volume element along a ray tube. The determinant $|U|$ vanishes near singular points of Λ, thus causing the blow-up of the amplitude near caustics.

At caustics where the geometrical optics amplitude blows up, the exact solution of Maxwell's Eq. (1) exhibits a large (but finite) peak of intensity. In optics, this phenomenon is very common and can be easily observed in "real life."[56] Typical examples are the bright spots on the bottom of a swimming pool due to the focusing effects of surface waves, or in a cup of coffee, due to the curvature of the inner surface of the cup.

From a physical point of view, the validity of geometrical optics has been investigated by Kravtsov and Orlov,[5,57] with the result that the geometrical optics solution (9) fails when wave effects such as diffraction[4] become important. This drawback can be cured by complex geometrical optics, as explained in Sec. II B.

In addition to its computational advantages, geometrical optics allows us to extract relevant physical information. Within the limits of applicability, i.e., when diffraction effects can be neglected, Eq. (5b) implies that the wave energy density is transported along geometrical optics rays. More specifically, Eq. (5b) can be recast in the form[5] (after some algebra and restoring dimensional quantities)

$$\nabla_r \cdot [v_g W] = -\gamma W, \tag{15}$$

where ∇_r denotes the gradient in physical (dimensional) coordinates,

$$v_g = -\frac{\partial H/\partial k}{\partial H/\partial\omega} = c\left|\frac{\partial(\omega H)}{\partial\omega}\right|^{-1}\frac{\partial H}{\partial N} \tag{16}$$

is the group velocity,[35] and

$$W = \left|\frac{\partial(\omega H)}{\partial\omega}\right|\frac{|A|^2}{16\pi} = \frac{1}{\omega}\left[e^* \cdot \frac{\partial(\omega^2\varepsilon_0)}{\partial\omega}e\right]\frac{|A^2|}{16\pi} \tag{17}$$

is the total wave energy density, comprising the electric, magnetic, and sloshing energy.[35,36] At last,

$$\gamma = \left|\frac{\partial(\omega H)}{\partial\omega}\right|^{-1} 2\gamma_1 \tag{18}$$

is the energy absorption coefficient. Here, all derivatives with respect to the frequency are taken at constant wave vector $k = \omega N/c$, and phase-space functions are evaluated at $N = \nabla S$.

The aim of this paper is the precise derivation of an energy conservation law analogous to (15) in the framework of complex geometrical optics.

B. Review of complex eikonal theory

Both cusped and folded singularities shown in Figure 1 are common in plasma physics application of high frequency beams. For example, focused beams are used either in diagnostics or heating in order to increase the localization of the measurement or power deposition, while folds are the essential components of reflectometry diagnostics.

Complex geometrical optics is a development of standard geometrical optics in which the eikonal function $S(x)$ in the ansatz (4) is replaced by a complex valued function $\psi(x) = S(x) + i\phi(x)$. With slight abuse of notation, it is customary to denote by $S(x)$ both the geometrical optics eikonal and the real part of the complex eikonal, although those are two different functions. The imaginary part ϕ accounts for the spatial inhomogeneity of the beams on a short scale. This will be made precise in Sec. II C.

In this section, we review the standard approach to the complex eikonal theory leading to the concept of extended rays. We follow the seminal paper by Choudhary and Felsen[27] and consider the Helmholtz equation for the scalar wave field $u(\kappa, x)$, namely,

$$[\Delta + \kappa^2 n^2(x)]u(\kappa, x) = 0,$$

where Δ is the Laplacian operator and $n(x)$ is the refractive index of the medium. The complex geometrical optics ansatz reads

$$u(\kappa, x) = e^{i\kappa\psi(x)}a(\kappa, x),$$

where $a(\kappa, x) \sim a_0(x) + \kappa^{-1}a_1(x) + \ldots$ as in Eq. (4). Upon substituting the ansatz into the Helmholtz equation, one finds that the leading order in the limit $\kappa \to +\infty$ is determined by

$$(\nabla\psi)^2 - n^2(x) = 0, \tag{19a}$$

$$2\nabla\psi \cdot \nabla a_0 + \Delta\psi a_0 = 0, \tag{19b}$$

which are formally identical to geometrical optics Eqs. (5) for the Hamiltonian (14) and $\gamma_1 = \delta_1 = 0$ as relevant to the Helmholtz equation. The only important difference is that $\psi(x)$ is now complex-valued.

One approach to the solution of (19) relies on the concept of complex rays, which consists essentially in using the theory of characteristics in the complex space.[19–21] The physical meaning of complex rays however is not evident and a different approach formulated entirely in the physical space has been developed. We shall focus on the latter.

Let us consider first Eq. (19a), which is referred to as complex eikonal equation. Separating its real and imaginary

parts yields the system of nonlinear partial differential equations

$$(\nabla S)^2 - (\nabla\phi)^2 - n^2(x) = 0, \tag{20a}$$

$$\nabla S \cdot \nabla\phi = 0. \tag{20b}$$

When $\nabla\phi$ is zero, the solution for S is expected to be the same as the solution of the corresponding eikonal equation $(\nabla S)^2 - n^2 = 0$, for which rays are tangent to the vector field $\nabla S(x)$, and thus normal to the $S =$ constant surfaces, i.e., the phase fronts. This is generalized to the case $\nabla\phi \neq 0$. Extended rays are defined as the curves tangent to the vector field ∇S. The name "extended rays" was proposed by Peeters.[32] As a consequence the function, ϕ is constant along an extended ray because of the orthogonality condition $\nabla S \cdot \nabla\phi = 0$.

Extended rays can still be computed via Hamilton's equation, but now the Hamiltonian

$$H_\phi(x,N) = N^2 - n^2(x) - (\nabla\phi(x))^2 \tag{21}$$

depends on the unknown function ϕ, which is reconstructed in numerical codes from the fact that ϕ is constant along extended rays.[1]

By inspection of the Hamiltonian, one can give an interpretation of the dynamics of extended rays as the motion of a point particle of mass $1/2$ in the potential $-n^2 - (\nabla\phi)^2$. The term $-n^2$ is the usual potential of geometrical optics, while $-(\nabla\phi)^2$ depends on neighboring rays. In typical situations, $\nabla\phi$ increases with the distance from the axis of the beam, hence $-(\nabla\phi)^2$ has a maximum on the beam axis and rays tends to be repelled from it. In the presence of focusing (cf. Figure 1 panels (a) and (b)), this effect becomes large in the focus and prevents rays to cross the beam axis, thus removing the singularity at the focal point.

This argument is purely qualitative. There is no *a priori* guarantee that, in general, the complex geometrical optics will not develop a singularity. For instance, in points where $\nabla S = 0$, there can be no real valued solution of the system (20). Moreover, for one dimensional problems, $S' \neq 0$ implies that ϕ is constant, so that the system (20) reduces to the standard eikonal equation for S. The introduction of a complex phase has no effect in one dimension as far as n^2 is real-valued, i.e., no dissipation at the leading order in κ is present.

The generalization of Eq. (20) to the case of anisotropic spatially non-dispersive media, i.e., to the case of Eq. (1), has been addressed by Mazzucato,[28] using the formal expansion

$$H(x,\nabla\psi) = H(x,\nabla S) + i\nabla\phi\cdot\nabla_N H(x,\nabla S) - \frac{1}{2}\nabla\phi\cdot D_N^2 H(x,\nabla S)\nabla\phi + \cdots,$$

where $H(x,\nabla\psi)$ is the geometrical optics Hamiltonian introduced in Sec. II A, analytically continued in the space of complex momenta, and $D_N^2 H(x,N) = (\partial^2 H(x,N)/\partial N_i \partial N_j)_{ij}$ is the Hessian matrix of H with respect to momenta. The expansion is formally justified by assuming the physical condition $|\nabla\phi| \ll |\nabla S|$. The real and imaginary parts define the systems

$$\begin{cases} H(x,\nabla S) - \dfrac{1}{2}\nabla\phi\cdot D_N^2 H(x,\nabla S)\nabla\phi = 0, \\ \nabla_N H(x,\nabla S)\cdot\nabla\phi = 0. \end{cases} \tag{22}$$

In this more general case, $\nabla\phi$ is orthogonal to the vector field $V(x) = \nabla_N H(x,\nabla S)$, which is defined as in geometrical optics, cf. Eq. (6), but with S obtained from the extended ray dynamics. Specifically, the Hamiltonian for extended rays is

$$H_\phi(x,N) = H(x,N) - \frac{1}{2}\nabla\phi(x)\cdot D_N^2 H(x,N)\nabla\phi(x), \tag{23}$$

and one can see that, in general, ϕ is not constant along extended rays. This is a complication in the numerical reconstruction of ϕ.

In the GRAY code,[1] the imaginary part ϕ of the phase is assumed to be constant along extended rays, a choice that greatly simplifies the derivation of a numerical scheme. This corresponds to adding a term proportional to $|\nabla\phi|^3$ to the second equation of (22), which is heuristically justified by invoking again the condition $|\nabla\phi| \ll |\nabla S|$.

In Sec. III, we propose a systematic approach, which provides a mathematically precise way to control the formal expansion in $\nabla\phi$ and applies even when the Hamiltonian $H(x,N)$ is not analytic in the argument N. In addition, our approach allows us to address the problem of ϕ being not exactly constant along extended rays.

On going back to Eq. (20b), we write

$$a_0(x) = A(x)e^{i\theta(x)},$$

where $A = |a_0|$ and $\theta = \arg a_0$ are real-valued, and we split the real and imaginary parts of the equation with the result that

$$2\nabla S\cdot\nabla A - 2(\nabla\phi\cdot\nabla\theta)A + \Delta S A = 0, \tag{24a}$$

$$2\nabla S\cdot\nabla\theta + 2(\nabla\phi\cdot\nabla A)/A + \Delta\phi = 0. \tag{24b}$$

This system of coupled partial differential equations determines the amplitude A and the phase shift θ of the wave field. In contrast to the geometrical optics transport Eq. (5b), this cannot be reduced to ordinary differential equations along rays. Indeed, the variations of A and θ in both the directions ∇S (tangent to extended rays) and $\nabla\phi$ (normal to extended rays in this case) are involved. The derivation of a conservation law of the form (15) is also not evident from the system (24).

We shall show in Sec. III that Eqs. (19) are unnecessarily too restrictive. By making use of a sharper control on the order of terms in the asymptotic expansion for the wave equation, we shall show that the terms proportional to $\nabla\phi$ can be neglected, thus obtaining a decoupled system of transport equations for the amplitude A and the phase θ.

C. Paraxial character of complex eikonal waves

Our main results of Sec. III rely on simple but important properties of complex eikonal wave fields that were observed independently by Pereverzev[9] and Maslov.[10] In this section,

we review such results, properly reformulated in order to apply to our framework.

We are interested in asymptotic solutions of Eq. (1) in the form of a complex eikonal wave field, namely,

$$E_{\mathrm{CGO}}(\kappa,x) = e^{i\kappa\psi(x)}a(\kappa,x), \tag{25a}$$

where $\psi(x) = S(x) + i\phi(x)$, $\phi(x) \geq 0$, is the complex eikonal,

$$a(\kappa,x) \sim a_0(x) + \kappa^{-1}a_1(x) + \cdots, \tag{25b}$$

and the amplitudes $a_j(x)$ are independent of κ and bounded in x with bounded derivatives. The asymptotic sum $a(\kappa,x)$ has been formally introduced in the standard eikonal ansatz (4). Here, we need some more information. According to the standard definition of asymptotic series,[37] the sum $a(\kappa,x)$ is not unique. Two asymptotic sums of the same sequence a_j differ for a remainder that is exponentially decreasing in the limit $\kappa \to +\infty$. One possible choice of $a(\kappa,x)$ is given by the sum of the series $\chi(\epsilon_j\kappa)\kappa^{-j}a_j(x)$ where the cut-off function $0 \leq \chi(\epsilon_j\kappa) \leq 1$ vanishes identically for $\epsilon_j\kappa \leq 1$, and ϵ_j is a sequence of positive numbers approaching zero monotonically. Hence, the sum $a(\kappa,x) = \sum_j \chi(\epsilon_j\kappa)\kappa^{-j}a_j(x)$ has only a finite number of terms for every κ and x. In addition, for bounded amplitudes $|a_j(x)| \leq C_j$, we have $|\chi(\epsilon_j\kappa)\kappa^{-j}a_j(x)| \leq \epsilon_j^j C_j$, and we can choose the sequence ϵ_j so that $\epsilon_j^j C_j \leq 1/j^2$. Since the series of $1/j^2$ is convergent, the asymptotic sum $a(\kappa,x)$ is bounded and we write

$$|a(\kappa,x)| \leq C_0, \quad \text{for } \kappa \geq \kappa_0,$$

where $C_0 > 0$ and $\kappa_0 > 0$ are constants. The condition $\phi(x) \geq 0$ on the imaginary part of the eikonal is required by the boundedness of the wave field for $\kappa \to +\infty$.

Ansatz (25) should now be substituted into the wave Eq. (1). Before proceeding, however, let us make two important observations, following the idea of Pereverzev[9] and Maslov.[10] Both are consequences of the condition $\phi(x) \geq 0$ and imply that the wave field (25a) is *paraxial*.

The first observation is that the wave field (25a) is exponentially small, in the limit $\kappa \to +\infty$ near points x where $\phi(x) > 0$. Indeed, one has $|E_{\mathrm{CGO}}(\kappa,x)| \propto e^{-\kappa\phi(x)} \to 0$ for $\kappa \to +\infty$. More precisely, for every integer $n > 0$,

$$\kappa^n |E_{\mathrm{CGO}}(\kappa,x)| \leq C_0 \left(\frac{n}{e\phi(x)}\right)^n, \quad \phi(x) > 0, \tag{26}$$

which is tantamount to exponential decay.

The second observation requires some preparation. Estimate (26) means that the wave field (25a), in the limit $\kappa \to +\infty$, collapses on the zero-level set of the function $\mathrm{Im}\psi = \phi$, namely,

$$\mathcal{R} = \{x;\ \phi(x) = 0\}. \tag{27}$$

We restrict our attention to cases in which $\mathcal{R}$ is a curve given parametrically by $x = \bar{x}(\tau)$. In the paraxial WKB theory, this is called reference ray.[9] Let us mention that it is possible to weaken this assumption and allow $\mathcal{R}$ to be a two-dimensional submanifold satisfying appropriate conditions, but this is hardly encountered in the applications (for the interested reader, this generalization is described in an unpublished note[58]).

By definition $\phi(\bar{x}(\tau)) = 0$, identically in τ and,

$$0 = \frac{d}{d\tau}\phi(\bar{x}(\tau)) = \frac{d\bar{x}(\tau)}{d\tau} \cdot \nabla\phi(\bar{x}(\tau)),$$

which means that the component of $\nabla\phi(\bar{x}(\tau))$ tangent to the curve $\mathcal{R}$ vanishes identically. The other two components must vanish as well, otherwise ϕ would change sign across $\mathcal{R}$, thus violating the condition $\phi \geq 0$. It follows that

$$\nabla\phi(\bar{x}(\tau)) = 0, \tag{28}$$

identically in τ. Then, the Taylor polynomial of ϕ around $\bar{x}$ has terms of second order or higher only. Continuing, one has

$$0 = \frac{d}{d\tau}\nabla\phi(\bar{x}(\tau)) = D^2\phi(\bar{x}(\tau))\frac{d\bar{x}(\tau)}{d\tau},$$

where $D^2\phi(x) = (\partial^2\phi(x)/\partial x^i \partial x^j)_{ij}$ is the Hessian matrix of second-order derivatives of ϕ. Therefore, the tangent vector $e_t(\tau) \propto d\bar{x}(\tau)/d\tau$ is an eigenvector of $D^2\phi(\bar{x}(\tau))$ corresponding to the null eigenvalue.

In general, the whole matrix $D^2\phi(\bar{x})$ can be zero and, in that case, the Taylor polynomial of ϕ would have only terms of fourth order or higher (the third order is again excluded by the condition $\phi \geq 0$). For definiteness, we shall consider the case in which, except for the tangent direction $\propto e_t$, the matrix $D^2\phi(\bar{x})$ is strictly positive definite. Precisely,

$$w \cdot D^2\phi(\bar{x}(\tau))w > 0, \tag{29}$$

for every vector w linearly independent of $e_t(\tau)$, i.e., $D^2\phi$ is positive definite for vectors transversal to the reference curve $\mathcal{R}$.

The exact Taylor formula for ϕ now reads

$$\phi(x) = \frac{1}{2}(x-\bar{x}) \cdot Q(x,\bar{x})(x-\bar{x}),$$

where, for $|x-\bar{x}|$ small enough, the symmetric matrix

$$Q(x,\bar{x}) = 2\int_0^1 D^2\phi((1-s)\bar{x} + sx)(1-s)ds$$

is positive definite for vectors transversal to the reference curve $\mathcal{R}$. Through diagonalization of the matrix Q, for every point x in a neighborhood of $\mathcal{R}$, one can find $\bar{x}$ on $\mathcal{R}$ for which there exists a $d \times d$ matrix $B(x,\bar{x})$ satisfying

$$(x-\bar{x}) \cdot Q(x,\bar{x})(x-\bar{x}) = (x-\bar{x}) \cdot {}^tB(x,\bar{x})B(x,\bar{x})(x-\bar{x}),$$

where ${}^tB$ denotes the transpose of B. With the new function $\xi(x) = B(x,\bar{x})(x-\bar{x})$, the imaginary part of the complex phase becomes

$$\phi(x) = \frac{1}{2}\xi(x)^2.$$

This form of the imaginary part ϕ is valid in a neighborhood of $\mathcal{R}$ only and it is of dubious practical utility, except for obtaining the following inequality:[9]

$$|\xi(x)^{\alpha}e^{-\kappa\phi(x)}| = |z^{\alpha}e^{-z^2/2}|\kappa^{-|\alpha|/2} \leq C_{\alpha}\kappa^{-|\alpha|/2},$$

where the multi-index notation has been used: the vector of integers $\alpha = (\alpha_1, \ldots, \alpha_d)$ is the multi-index, with length $|\alpha| = \alpha_1 + \cdots + \alpha_d$, and $\xi^{\alpha} = (\xi^1)^{\alpha_1}, \ldots, (\xi^d)^{\alpha_d}$. Here, $z = \sqrt{\kappa}\xi$ and $C_{\alpha} > 0$ is a constant depending only on α. Roughly speaking, every time one multiplies the exponential $e^{-\kappa\phi}$ by any component ξ^i, the order is reduced by a factor $1/\sqrt{\kappa}$. On noting that $\nabla\phi(x) = \delta_{ij}(\nabla\xi^i(x))\xi^j(x)$, one has

$$|(\nabla\phi)^{\alpha}e^{i\kappa\psi}| \leq C_{\alpha}\kappa^{-|\alpha|/2}, \tag{30}$$

where C_{α} is a different constant. This is the second consequence of the ansatz (25a).

Differently from estimate (26) however, (30) is not fully general as it relies on the assumptions that (i) the set (27) is a curve, and (ii) the matrix $D^2\phi$ satisfies (29). The latter condition, in particular, is the reason for which half-integer powers of $1/\kappa$ are found. We shall see that this is the appropriate setting for studying focused beams, for which the caustic geometry is similar to the one represented in Figures 1(a) and 1(b). This is the situation of practical interest for electromagnetic wave beams in fusion plasmas, including focused beams. However, the assumptions on the topology of the set $\mathcal{R}$ and on the Hessian matrix $D^2\phi$ are not general enough to cope with arbitrary caustic singularities. When a folded singularity is present, like for instance in the cases of Figures 1(c) and 1(d), the asymptotic expansion of the wave field is obtained in powers of $\kappa^{1/3}$, cf. Sec. 3.4 of Babič and Buldyrev,[4] and near the cut-off such ordering should be properly accounted for.

III. COMPLEX GEOMETRICAL OPTICS EQUATIONS, EXTENDED RAYS, AND WAVE ENERGY TRANSPORT

The estimates reviewed in Sec. II C are now applied to the derivation of complex geometrical optics equations. Our approach is characterized by a sharper control of terms in the asymptotic expansion of the wave equation in the limit $\kappa \to +\infty$. As anticipated above, this will eventually lead to a simplified form of the amplitude transport equation, which in turns yields the energy continuity equation.

The first part of the derivation follows the standard one reviewed in Sec. II B. The complex eikonal ansatz (25) is substituted into Maxwell's Eq. (1), and the asymptotic expansion is performed in the limit $\kappa \to +\infty$. Thereafter, the analysis of the resulting equation is different. In order to keep the paper self-contained, the whole procedure is described in details.

A. Complex eikonal theory

The substitution of the ansatz (25a) into Maxwell's wave Eq. (1) for the electric field yields

$$e^{i\kappa\psi}\left\{\kappa^2\mathsf{D}_0(x,\nabla\psi)a_0(x) + \kappa\left[\mathsf{D}_0(x,\nabla\psi)a_1 - i\left[\frac{\partial\mathsf{D}_0}{\partial N_i}(x,\nabla\psi)\frac{\partial a_0}{\partial x^i} + \frac{1}{2}\frac{\partial}{\partial x^i}\left[\frac{\partial\mathsf{D}_0}{\partial N_i}(x,\nabla\psi)\right]a_0 - i\varepsilon_1 a_0\right]\right]\right\} + O(1) = 0, \tag{31}$$

where Eq. (2) has been accounted for. In writing Eq. (31), one should note that the dispersion tensor D_0, defined in Eq. (3), is a polynomial in N and it extends to an entire function of the complex refractive index $\tilde{N} = N + iN'$. We can, therefore, evaluate D_0 at $\tilde{N} = \nabla\psi$. The same argument applies to the derivatives of D_0. Explicitly,

$$\mathsf{D}_{0,ij}(x,\nabla\psi) = (\nabla\psi)^2\delta_{ij} - \frac{\partial\psi}{\partial x^i}\frac{\partial\psi}{\partial x^j} - \varepsilon_{0,ij}(x), \tag{32a}$$

$$\frac{\partial\mathsf{D}_{0,ij}}{\partial N_k}(x,\nabla\psi) = 2\frac{\partial\psi}{\partial x^l}\delta^{lk}\delta_{ij} - \delta_i^k\frac{\partial\psi}{\partial x^j} - \frac{\partial\psi}{\partial x^i}\delta_j^k, \tag{32b}$$

$$\frac{\partial^2\mathsf{D}_{0,ij}}{\partial N_k\partial N_l}(x,\nabla\psi) = 2\delta^{kl}\delta_{ij} - \delta_i^k\delta_j^l - \delta_i^l\delta_j^k, \tag{32c}$$

while

$$\frac{\partial}{\partial x^k}\left[\frac{\partial\mathsf{D}_{0,ij}}{\partial N_k}(x,\nabla\psi)\right] = \frac{\partial^2\mathsf{D}_{0,ij}}{\partial x^k\partial N_k}(x,\nabla\psi) + \frac{\partial^2\psi}{\partial x^k\partial x^l}\frac{\partial^2\mathsf{D}_{0,ij}}{\partial N_k\partial N_l}(x,\nabla\psi). \tag{33}$$

The first term on the right-hand side of (33) is actually zero for the dispersion tensor (3), and the second-order derivative with respect to N is constant, cf. Eq. (32c). In the following, we keep both terms formally general. This will be needed for spatially dispersive media in Sec. V.

When one neglects the paraxial character of the wave field discussed in Sec. II C, terms of different order in κ are separated in (31), yielding a hierarchy of equations for ψ, a_0, and a_1. Such equations, although formally similar to the corresponding equations of standard geometrical optics,[38] are complicated by the presence of the imaginary part of the phase. The hierarchy thus obtained, however, is unnecessarily too strong and it can be considerably simplified by taking into account inequalities (26) and (30).

Inequality (30) in particular implies that terms proportional to $\mathrm{Im}\nabla\psi = \nabla\phi$ in Eq. (31) can be better estimated by half-integer powers of κ.

When that is accounted for, Eq. (31) becomes

$$e^{i\kappa\psi}\left\{\kappa^2\mathsf{D}_0(x,\nabla\psi)a_0(x) + \kappa\left[\mathsf{D}_0(x,\nabla S)a_1 - i\left[\frac{\partial\mathsf{D}_0}{\partial N_i}(x,\nabla S)\frac{\partial a_0}{\partial x^i} + \frac{1}{2}\left[\frac{\partial^2\mathsf{D}_0}{\partial x^i\partial N_i}(x,\nabla S) + \frac{\partial^2\psi}{\partial x^i\partial x^j}\times\frac{\partial^2\mathsf{D}_0}{\partial N_i\partial N_j}(x,\nabla S)\right]a_0 - i\varepsilon_1 a_0\right]\right]\right\} + O(\sqrt{\kappa}) = 0. \tag{34}$$

Now the imaginary part of the complex phase enters the $O(\kappa)$-term through the Hessian matrix $\partial^2\psi/\partial x^i\partial x^j$ only, a simplification which will be crucial in deriving the wave energy flux.

The asymptotic expansion (34) of the wave equation is solved within an $O(\sqrt{\kappa})$ residual, which corresponds to an error of $O(\kappa^{-3/2})$ as the leading terms in the wave equation are quadratic in κ.

We can now exploit the linear independence of monomials κ^n and separate the coefficients of κ^2 and κ. In view of estimate (30) however, a remainder of appropriate order in $\nabla\phi$ can be allowed in the equations thus obtained. Specifically,

$$\mathsf{D}_0(x,\nabla\psi)a_0 = \rho_0(x,\nabla\phi), \tag{35a}$$

$$\mathsf{D}_0(x,\nabla S)a_1 - i\left[\frac{\partial \mathsf{D}_0}{\partial N_i}(x,\nabla S)\frac{\partial a_0}{\partial x^i} + \frac{1}{2}\left[\frac{\partial^2 \mathsf{D}_0}{\partial x^i \partial N_i}(x,\nabla S) + \frac{\partial^2\psi}{\partial x^i\partial x^j}\frac{\partial^2 \mathsf{D}_0}{\partial N_i \partial N_j}(x,\nabla S)\right]a_0 - i\varepsilon_1 a_0\right] = \rho_1(x,\nabla\phi), \tag{35b}$$

where the remainders ρ_0 and ρ_1 must be at least cubic and linear in $\nabla\phi$, respectively. Let us remark that this is not a perturbative argument in $\nabla\phi$: In general, the remainders are by no means small, except in a narrow strip around the zero-level set (27), where the beam is localized.

Since the remainders ρ_0 and ρ_1 are arbitrary, any term of order $|\nabla\phi|^3$ and $|\nabla\phi|$ can be added to (35a) and (35b), respectively, without changing the order of the residual in the wave equation.

If we can find the solution of such equations for ψ, a_0, and a_1, then the coefficient of κ^2 in the asymptotic form (34) of the wave equation can be substituted by the cubic remainder ρ_0, and, analogously, the coefficient of κ can be replaced by ρ_1. Equation (30), in conclusion, shows that the result is of $O(\sqrt{\kappa})$, which is the desired residual.

1. Solution of equation (35a)

The matrix $\mathsf{D}_0(x,\nabla\psi)$ is no longer Hermitian, even though $\mathsf{D}_0(x,N)$ is Hermitian for a real valued refractive index N. Nonetheless, $\mathsf{D}_0(x,\nabla\psi)$ is much simpler than a generic complex matrix, as it is the analytical continuation of a Hermitian matrix.

For the specific case of the dispersion tensor (3), one can check, e.g., by means of (32), that the identity,

$$\mathsf{D}_0(x,\tilde{N}) = \tilde{\mathsf{D}}_0(x,\tilde{N}),$$

holds true with $\tilde{N} = N + iN'$ and

$$\tilde{\mathsf{D}}_0(x,\tilde{N}) = \mathsf{D}_0(x,N) + i\frac{\partial \mathsf{D}_0(x,N)}{\partial N_k}N_k' - \frac{1}{2}\frac{\partial^2 \mathsf{D}_0(x,p)}{\partial N_k \partial N_l}N_k'N_l'.$$

This defines a convenient complex extension of $\mathsf{D}_0(x,N)$ up to second-order terms in the imaginary part N'. Such an apparently cumbersome way of rewriting $\mathsf{D}_0(x,\tilde{N})$ allows us to exploit the properties of the Hermitian matrix $\mathsf{D}_0(x,N)$. Besides, the form $\tilde{\mathsf{D}}_0(x,\tilde{N})$ is naturally encountered for the case of spatially dispersive media treated in Sec. V.

Consistently, given an eigenvector $e_j(x,N)$ of the Hermitian matrix $\mathsf{D}_0(x,N)$ corresponding to the eigenvalue $\lambda_j(x,N)$, we define the complex extension of e_j by an analogous expression,

$$\tilde{e}_j(x,\tilde{N}) = e_j(x,N) + i\frac{\partial e_j(x,N)}{\partial N_k}N_k' - \frac{1}{2}\frac{\partial^2 e_j(x,N)}{\partial N_k \partial N_l}N_k'N_l', \tag{36}$$

as well as the complex extension of its dual,

$$\tilde{f}_j(x,\tilde{N}) = e_j^*(x,N) + i\frac{\partial e_j^*(x,N)}{\partial N_k}N_k' - \frac{1}{2}\frac{\partial^2 e_j^*(x,N)}{\partial N_k \partial N_l}N_k'N_l', \tag{37}$$

and the complex extension of the corresponding eigenvalue,

$$\tilde{\lambda}_j(x,\tilde{N}) = \lambda_j(x,N) + i\frac{\partial \lambda_j(x,N)}{\partial N_k}N_k' - \frac{1}{2}\frac{\partial^2 \lambda_j(x,N)}{\partial N_k \partial N_l}N_k'N_l', \tag{38}$$

where again $\tilde{N} = N + iN'$. (A mathematically complete presentation of this argument can be found in the unpublished note[58] quoted above.)

Upon taking into account the eigenvalue equation $\mathsf{D}_0 e_j = \lambda_j e_j$, together with its derivatives with respect to N, one gets the identity

$$\tilde{\mathsf{D}}_0(x,\tilde{N})\tilde{e}_j(x,\tilde{N}) - \tilde{\lambda}_j(x,\tilde{N})\tilde{e}_j(x,\tilde{N}) = O(|N'|^3), \tag{39}$$

which shows that $\tilde{e}_j(x,\tilde{N})$ is an eigenvector of $\tilde{\mathsf{D}}_0(x,\tilde{N})$ with eigenvalue $\tilde{\lambda}_j(x,\tilde{N})$, apart from an $O(|N'|^3)$ remainder.

Identity (39) implies that Eq. (35a) is solved by a complex eikonal $\psi(x)$ and an amplitude $a_0(x)$ such that

$$\tilde{H}(x,\nabla\psi) = \sigma_0(x,\nabla\phi), \tag{40a}$$

$$a_0(x) = A(x)\tilde{e}(x,\nabla\psi), \tag{40b}$$

where $\tilde{H}(x,\tilde{N})$ is the complex extension of the specific eigenvalue $H(x,N)$ relevant to the considered wave mode, $\sigma_0(x,\nabla\phi)$ is an arbitrary cubic remainder, $\tilde{e}(x,\tilde{N})$ is the complex extension of the corresponding eigenvector, and $A(x)$ is an arbitrary complex scalar amplitude.

Given the wave mode, solution (40a) is indeed the only possible solution of (35a). In order to see that, let us recall that the eigenvectors of a Hermitian matrix are complete, i.e., they span the whole space. This is expressed by the identity

$$I = \sum_j e_j(x,N)e_j^*(x,N), \tag{41}$$

which holds true for every (x,N) in the wave phase space. Here, I is the identity matrix. By taking into account (41)

and its derivatives with respect to N, one can check that the completeness relation holds for complex extended quantities as well, but with a usual cubic remainder, namely,

$$I - \sum_j \tilde{e}_j(x,\tilde{N})\tilde{f}_j(x,\tilde{N}) = O(|N'|^3). \tag{42}$$

In the same way, one can extend the orthogonality of eigenvectors, namely, $e_i^*(x,N)\cdot e_j(x,N) = \delta_{ij}$, which reads

$$\tilde{f}_i \cdot \tilde{e}_j - \delta_{ij} = O(|N'|^3). \tag{43}$$

Then, a generic amplitude vector can be written in the form

$$\begin{aligned} a_0(x) &= \sum_j \tilde{e}_j(x,\nabla\psi)(\tilde{f}_j(x,\nabla\psi)\cdot a_0(x)) + O(|\nabla\phi|^3), \\ &= \sum_j A_j(x)\tilde{e}_j(x,\nabla\psi) + O(|\nabla\phi|^3), \end{aligned}$$

and Eq. (35a) amounts to

$$\sum_j \tilde{\lambda}_j(x,\nabla\psi)A_j(x)\tilde{e}_j(x,\nabla\psi) + O(|\nabla\phi|^3) = \rho_0(x,\nabla\phi).$$

One can now apply $\tilde{f}_i$ on the left and use the orthogonality (43), thus splitting the vector Eq. (35a) into three scalar equations,

$$\tilde{\lambda}_i(x,\nabla\psi)A_i(x) + O(|\nabla\phi|^3) = \tilde{f}_i(x,\nabla\psi)\cdot\rho_0(x,\nabla\phi),$$

for $i = 1,2,3$. The amplitude A_i can be different from zero only if $\tilde{\lambda}_i(x,\nabla\psi) = O(|\nabla\phi|^3)$. On the other hand, only one out of the three eigenvalues can fulfill this condition for a given complex phase ψ, otherwise the hypothesis of separability of eigenvalues λ_j stated in Sec. II A would be violated in points $(x,\nabla S(x))$, $S = \mathrm{Re}\psi$, for $x = \bar{x}(\tau)$, i.e., on the reference curve (27). It follows that, given a specific wave mode corresponding to a specific eigenvalue H, Eq. (40a) gives the only solution for that mode.

Equation (40a) depends on the arbitrary cubic remainder σ_0, and therefore it does not determine uniquely the complex eikonal ψ. Such a loss of uniqueness is a natural consequence of fixed-order asymptotics. Since we require that the wave equation is solved up to a fixed order ($O(\sqrt{\kappa})$ in this case), we cannot distinguish between two different complex phases that produce the same leading order terms in the wave equation.

With the natural choice $\sigma_0(x,\nabla\phi) = 0$, Eq. (40a) reduces to the system (22) obtained by Mazzucato and discussed in Sec. II B. Hence, we have recovered the standard equations for extended rays, but without the need for the condition $|\nabla\phi| \ll |\nabla S|$.

As already discussed in Sec. II B, in the standard extended ray theory, one identifies two vector fields. The first field is

$$V(x) = \frac{\partial H}{\partial N}(x,\nabla S(x)), \tag{44}$$

along which ϕ is constant. This is formally the same as the vector field (6) defined in geometrical optics, but the analogy is purely formal. Indeed, the function S here is coupled to ϕ and therefore differs from the corresponding quantity in the standard geometrical optics. This coupling between S and ϕ introduces wave effects. The second vector field is

$$\begin{aligned} V_\phi(x) &= \frac{\partial H_\phi}{\partial N}(x,\nabla S(x)) \\ &= V(x) - \frac{1}{2}\frac{\partial\phi}{\partial x^k}\frac{\partial\phi}{\partial x^l}\frac{\partial^3 H}{\partial N\partial N_k\partial N_l}(x,\nabla S), \end{aligned} \tag{45}$$

which is tangent to extended rays. Here, H_ϕ is the Hamiltonian of extended rays defined in Eq. (23).

A special case of particular interest is that of Hamiltonians depending quadratically on momenta. Since the third derivatives $\partial^3 H/\partial N_i\partial N_j\partial N_k$ vanish identically, one has $V(x) = V_\phi(x)$ and ϕ is constant along extended rays. As an example, this is the case for isotropic spatially non-dispersive media.

In general, $\nabla\phi$ is small near the zero-level set $\mathcal{R}$ where the field is localized and the two vector fields are close one to the other, although differences can be present away from $\mathcal{R}$. For an efficient numerical implementation of extended ray equations, the conservation of ϕ along rays is a major simplification, and thus V is approximated by V_ϕ in the GRAY code,[1] cf. Sec. II B.

We propose here to exploit the freedom in selecting the remainder σ_0 in order to improve the geometrical properties of extended rays. Specifically, we can set

$$\sigma_0(x,\nabla\phi) = \frac{i}{2}\frac{\partial^3 H(x,\nabla S)}{\partial N_i\partial N_j\partial N_k}\frac{\partial\phi}{\partial x^i}\frac{\partial\phi}{\partial x^j}\frac{\partial\phi}{\partial x^k},$$

which is cubic in $\nabla\phi$ as required. Then, after the separation of the real and imaginary parts, Eq. (40a) takes the form

$$\begin{cases} H_\phi(x,\nabla S) = 0, \\ V_\phi(x)\cdot\nabla\phi = 0. \end{cases} \tag{46}$$

In this form, extended rays are still determined by the Hamiltonian (23) but now ϕ is exactly conserved by the extended ray flow. This provides a rigorous justification of the algorithm used in GRAY, which actually solves system (46).

2. Solution of equation (35b)

For the leading order Eq. (35a), our approach just allows us to recover known results in a systematic way. For Eq. (35b), on the contrary, we find significant simplifications. Removing the unnecessary high-order terms resulted in a simpler dependence of (35b) on the imaginary part of the phase. Such simplifications are pivotal in obtaining the wave energy flux.

On the line of the standard geometrical optics theory, let us first note a necessary condition for the existence of a solution of (35b).

Upon multiplication on the left by the complex extension $\tilde{f}$ of the dual eigenvector e^*, and noting that

$$\begin{aligned} &\tilde{f}(x,\nabla\psi)\cdot\mathsf{D}_0(x,\nabla\psi)a_1(x) \\ &\quad = \tilde{H}(x,\nabla\psi)\tilde{f}(x,\nabla\psi)\cdot a_1(x) + O(|\nabla\phi|^3), \end{aligned}$$

Eq. (35b) implies,

$$e^* \cdot \left[\frac{\partial \mathsf{D}_0}{\partial N_i} \frac{\partial [A\tilde{e}(x, \nabla\psi)]}{\partial x^i} + \frac{1}{2} \left[\frac{\partial^2 \mathsf{D}_0}{\partial x^i \partial N_i} + \frac{\partial^2 \psi}{\partial x^i \partial x^j} \frac{\partial^2 \mathsf{D}_0}{\partial N_i \partial N_j} \right] eA - i\varepsilon_1 eA \right] + O(|\nabla\phi|) = \tilde{f}(x, \nabla\psi) \cdot \rho_1(x, \nabla\psi), \tag{47}$$

where all phase space functions, when not explicitly indicated, are assumed to be evaluated at $(x, \nabla S)$, and the notation $\partial[\cdots]/\partial x^k$ denotes the derivative with respect to both the explicit and implicit dependence on x. Here, the term involving the derivative of $\tilde{e}$ must be dealt with carefully. From definition (36), one gets

$$\frac{\partial [A\tilde{e}]}{\partial x^k} = \frac{\partial [Ae]}{\partial x^k} + iA \frac{\partial e}{\partial N_l} \frac{\partial^2 \phi}{\partial x^k \partial x^l} + O(|\nabla\phi|),$$

hence

$$e^* \cdot \frac{\partial \mathsf{D}_0}{\partial N_k} \frac{\partial [A\tilde{e}]}{\partial x^k} = e^* \cdot \frac{\partial \mathsf{D}_0}{\partial N_k} \frac{\partial [Ae]}{\partial x^k} + \frac{iA}{2} e^* \cdot \left(\frac{\partial \mathsf{D}_0}{\partial N_l} \frac{\partial e}{\partial N_k} + \frac{\partial \mathsf{D}_0}{\partial N_k} \frac{\partial e}{\partial N_l} \right) \frac{\partial^2 \phi}{\partial x^k \partial x^l} + O(|\nabla\phi|). \tag{48}$$

The term in round brackets can be computed by making use of the identity obtained by deriving twice the eigenvalue equation $\mathsf{D}_0 e = He$ with respect to N, evaluating the result for $N = \nabla S$, and recalling that $H(x, \nabla S) = O(|\nabla\phi|^2)$, in virtue of the real part of Eq. (40a). That reads

$$e^* \cdot \left(\frac{\partial \mathsf{D}_0}{\partial N_l} \frac{\partial e}{\partial N_k} + \frac{\partial \mathsf{D}_0}{\partial N_k} \frac{\partial e}{\partial N_l} \right) = \frac{\partial^2 H}{\partial N_l \partial N_k} - e^* \cdot \frac{\partial^2 \mathsf{D}_0}{\partial N_l \partial N_k} e + e^* \cdot \left(\frac{\partial H}{\partial N_l} \frac{\partial e}{\partial N_k} + \frac{\partial H}{\partial N_k} \frac{\partial e}{\partial N_l} \right) + O(|\nabla\phi|^2).$$

After substituting the latter identity into (48), we estimate

$$\frac{\partial H}{\partial N_k} \frac{\partial^2 \phi}{\partial x^k \partial x^l} = -\frac{\partial V^k}{\partial x^l} \frac{\partial \phi}{\partial x^k} + O(|\nabla\phi|^2) = O(|\nabla\phi|),$$

which follows by applying $\partial/\partial x^l$ to the imaginary part of Eq. (40a). Then, (48) becomes

$$e^* \cdot \frac{\partial \mathsf{D}_0}{\partial N_k} \frac{\partial [A\tilde{e}]}{\partial x^k} = e^* \cdot \frac{\partial \mathsf{D}_0}{\partial N_k} \frac{\partial [Ae]}{\partial x^k} + \frac{iA}{2} \left[\frac{\partial^2 H}{\partial N_l \partial N_k} - e^* \cdot \frac{\partial^2 \mathsf{D}_0}{\partial N_l \partial N_k} e \right] \frac{\partial^2 \phi}{\partial x^k \partial x^l} + O(|\nabla\phi|).$$

And Eq. (47) reads

$$e^* \cdot \frac{\partial \mathsf{D}_0}{\partial N_k} \frac{\partial [Ae]}{\partial x^k} + e^* \cdot \left[\frac{1}{2} \frac{\partial}{\partial x^k} \left[\frac{\partial \mathsf{D}_0}{\partial N_k} \right] - i\varepsilon_1 \right] eA + \frac{i}{2} \frac{\partial^2 H}{\partial N_l \partial N_k} \frac{\partial^2 \phi}{\partial x^l \partial x^k} A + O(|\nabla\phi|) = \tilde{f} \cdot \rho_1. \tag{49}$$

One can note that the first two terms in Eq. (49) are formally the same as those in the corresponding equation of standard geometrical optics, which implies the transport Eq. (5b). The only difference consists in evaluating all phase space functions at $N = \nabla S$, with $\psi = S + i\phi$ solving (40a). Thus, one has $H(x, \nabla S) = O(|\nabla\phi|^2)$ as opposite to the exact local dispersion relation (5a) of the standard geometrical optics. With that in mind, we can follow the lines of the standard theory (cf., for instance Littlejohn and Flynn[38] and references therein), so that

$$e^* \cdot \frac{\partial \mathsf{D}_0}{\partial N_k} \frac{\partial [Ae]}{\partial x^k} + e^* \cdot \left[\frac{1}{2} \frac{\partial}{\partial x^k} \left[\frac{\partial \mathsf{D}_0}{\partial N_k} \right] - i\varepsilon_1 \right] eA = \frac{\partial H}{\partial N_k} \frac{\partial A}{\partial x^k} + \left[\frac{1}{2} \frac{\partial}{\partial x^k} \left[\frac{\partial H}{\partial N_k} \right] + \gamma_1 - i\delta_1 \right] A + O(|\nabla\phi|),$$

where, in particular, the identity (obtained by differentiating the real part of Eq. (40a)),

$$\frac{\partial H}{\partial x^k} + \frac{\partial^2 S}{\partial x^k \partial x^l} \frac{\partial H}{\partial N_l} = O(|\nabla\phi|),$$

has been accounted for. Thereby, one can see that Eq. (49) is equivalent to

$$V(x) \cdot \nabla A(x) - [-\gamma_1(x) + i(\delta_1(x) - \delta_{\text{Gouy}}(x)) - \frac{1}{2} \nabla \cdot V(x)] A(x) = \sigma_1(x, \nabla\phi), \tag{50}$$

where the vector field $V(x)$ is now given by (44), whereas γ_1 and δ_1 are formally given by (7) and (8), respectively. In complex eikonal theory, an additional phase shift is found, namely,

$$\delta_{\text{Gouy}}(x) = \frac{1}{2} \frac{\partial^2 H(x, \nabla S)}{\partial N_k \partial N_l} \frac{\partial^2 \phi}{\partial x^k \partial x^l}, \tag{51}$$

which is the generalization of the classical Gouy shift[59] and it is entirely due to diffraction effects. Again, we find an arbitrary remainder $\sigma_1(x, \nabla\phi)$, which must be at least linear in $\nabla\phi$.

Equation (50) describes the transport of the amplitude A that was left unspecified in Eqs. (40). Once Eq. (50) has been solved for the amplitude $A(x)$, one can show that the algebraic equation for a_1 has a solution, by means of an argument analogous to the uniqueness proof for (40), exploiting the completeness and orthogonality relations (42) and (43). As usual, such solution is never computed in practice, hence, we shall not digress on the details.

As for Eq. (40a), the actual calculation of the amplitude depends on the choice of the remainder σ_1.

The natural choice $\sigma_1 = 0$ gives the amplitude transport equation

$$V \cdot \nabla A = [-\gamma_1 + i(\delta_1 - \delta_{\text{Gouy}}) - \frac{1}{2} \nabla \cdot V] A, \tag{52}$$

describing the transport of the amplitude along the field lines of the vector $V(x)$. This is formally the same as the standard geometrical optics transport Eq. (5b), the only difference coming from the function S. In this case, the amplitude is not transported along extended rays.

Again we can improve the geometric properties of the transport equation by an appropriate choice of the linear remainder σ_1. One can check that

$$\sigma_1 = (V - V_\phi)\cdot\nabla A + \frac{1}{2}\nabla\cdot(V - V_\phi)A$$

is linear in $\nabla\phi$, and it is, therefore, a good choice for the remainder. Correspondingly, Eq. (50) takes the form

$$V_\phi\cdot\nabla A = [-\gamma_1 + i(\delta_1 - \delta_{\text{Gouy}}) - \frac{1}{2}\nabla\cdot V_\phi]A, \tag{53}$$

which describe the amplitude transport along extended rays.

Both Eqs. (52) and (53) implies the continuity equation for the approximated wave energy flux, cf. Sec. III B. We shall see that the energy fluxes obtained from such transport equations tend to the same limit for $\kappa \to +\infty$, but they are different for finite values of κ. In the latter case, we give quantitative estimates of the difference in Sec. IV.

3. Complex geometrical optics estimate of the residual

We can now formulate the main result of the foregoing asymptotic construction as an estimate of the residual in the wave equation.

Let $\psi = S + i\phi$ be a regular solution of Eq. (40a), and let a_0 be given in (40b), with $A(x)$ a regular solution of the complex geometrical optics transport Eq. (50). Then, it is possible to find a corrector a_1 such that the complex eikonal wave (25) solves the wave Eq. (1) for the electric field within an error,

$$|\kappa^{-2}\nabla\times\nabla\times E_{\text{CGO}}(\kappa,x) - \varepsilon(\kappa,x)E_{\text{CGO}}(\kappa,x)| \le C\kappa^{-3/2}. \tag{54}$$

As for the case of error estimate (10), this does not provide information on the convergence of E_{CGO} to the exact solution. Moreover, it relies on the existence of regular solutions for the complex eikonal ψ and amplitude A. When such solutions break down, estimate (54) fails to be uniform.

On the other hand, the coupling of the real phase S to the imaginary part ϕ successfully removes caustic singularities, at least, for the case of focalized beams, as shown by numerical results.[1,27–29,60]

At last, let us notice that the residual estimate (54) does not depend on the choice of the remainders σ_i, $i = 0, 1$, in Eqs. (40a) and (50).

B. Wave energy density flux

Let us start from Eq. (52), obtained for the natural choice of the remainder.

One of the advantages of our approach is that the transport Eq. (50) for the wave amplitude $A(x)$ parallels the corresponding transport equation in the standard geometrical optics, cf. Eq. (5b).

The only additional term in the complex geometrical optics transport equation is the Gouy phase shift, and a phase shift does not affect the transport of $|A|^2$, which reads

$$\nabla\cdot[V(x)|A(x)|^2] = -2\gamma_1(x,\nabla S)|A(x)|^2. \tag{55}$$

In complex geometrical optics however, the squared amplitude $|A|^2$ does not account for the whole electric field amplitude as, from (25) and (40),

$$|E_{\text{CGO}}(\kappa,x)|^2 = e^{-2\kappa\phi}|A(x)|^2 + O(1/\sqrt{\kappa}). \tag{56}$$

On the other hand, for the natural choice of both remainders σ_i, the orthogonality $V\cdot\nabla\phi = 0$ is satisfied, hence

$$\begin{aligned}\nabla\cdot[V(x)e^{-2\kappa\phi}|A|^2] &= e^{-2\kappa\phi}\nabla\cdot[V(x)|A|^2]\\ &\quad - 2\kappa e^{-2\kappa\phi}|A|^2 V\cdot\nabla\phi\\ &= e^{-2\kappa\phi}\nabla\cdot[V(x)|A|^2].\end{aligned}$$

Upon using this into Eq. (55), one finds that, formally, the standard geometrical optics energy transport Eqs. (15)–(18) hold true for complex geometrical optics as well, with only one modification in the definition of the wave energy density, namely,

$$W = \frac{1}{16\pi}\left|\frac{\partial(\omega H)}{\partial\omega}\right| e^{-2\kappa\phi}|A|^2, \tag{57}$$

where, we recall, the derivative $\partial/\partial\omega$ should be computed at constant wave vector $k = \omega N/c$. In complex geometrical optics, however, the coefficients of the transport Eq. (15) should be evaluated at $N = \nabla S$, where now S is the solution of the system (22).

The group velocity, in particular, is

$$v_g = c\left|\frac{\partial(\omega H)}{\partial\omega}\right|^{-1} V(x) \tag{58}$$

with $V(x)$ being the vector field defined in (44). One can conclude that, with the natural choice of both remainders σ_i, the wave energy density flow is approximated by the flow of the vector field $V(x) = \partial H(x,\nabla S)/\partial N$, and this can deviate from the corresponding geometrical optics quantity, due to diffraction effects. In general, the vector field V is not tangent to extended rays.

The mismatch between the approximated wave energy flow and the extended ray flow is removed in the optimized form of extended ray Eqs. (46) complemented with the transport Eq. (53). One can check that the above calculation holds true for the optimized formulation as well, yielding the energy transport equation in the form (15) with the group velocity given by

$$v_g = c\left|\frac{\partial(\omega H)}{\partial\omega}\right|^{-1} V_\phi(x), \tag{59}$$

which is now directed along extended rays. This result shows that extended rays computed according to (46) provide an approximation of the energy flow of the complex geometrical optics solution.

Let us remark that the energy continuity equation with either (58) or (59) is proven by making used of the condition $V\cdot\nabla\phi = 0$ and $V_\phi\cdot\nabla\phi = 0$, respectively. Therefore, the form (58) of the group velocity is appropriate to the standard formulation (Eq. (22)), while the form (59) is appropriate to the optimized formulation (Eq. (46)) and they cannot be exchanged.

In order to complete our analysis, we shall now show that, in both formulations, the quantity Wv_g converges to the

same limit for $\kappa \to +\infty$, as it should be, despite the vector field v_g is independent on κ. Then, we shall see that in both cases, Wv_g approximates the Poynting flux corresponding to the complex eikonal wave field.

The first claim is readily proven. In the limit $\kappa \to +\infty$, the wave energy density is supported on the reference ray where both vector fields $V(x)$ and $V_\phi(x)$ are the same. More precisely, given a complex eikonal $\psi = S + i\phi$, computed by either of the two formulations, let us consider the vector fields $V(x)$ and $V_\phi(x)$ computed via Eqs. (44) and (45) with the same complex eikonal ψ. Then estimate (30) implies that

$$|(V(x) - V_\phi(x))e^{-2\kappa\phi}| \le C/\kappa, \tag{60}$$

where $C > 0$ is a generic constant. This shows in particular that differences between the energy flux and the extended ray velocity in the standard formulation, Eq. (22), become small in the high frequency limit.

As for the Poynting flux, let us consider the conserved flux naturally implied by Eq. (1), namely,

$$F(\kappa, x) = \frac{2}{\kappa}\mathrm{Im}[E^*(\kappa, x) \times (\nabla \times E(\kappa, x))]. \tag{61}$$

Using (1) and (2), one finds

$$\nabla \cdot F = -2E^* \cdot \varepsilon_1^a E,$$

which shows that F is a conserved flux in a non-dissipative medium ($\varepsilon_1^a = 0$). Indeed, F is the normalized Poynting flux,[61] time-averaged over the period $2\pi/\omega$ of the beam (using harmonic field $E(t, x) = \mathrm{Re}\{e^{-i\omega t}E(\kappa, x)\}$).

For the specific case of a complex eikonal wave (25) with amplitude given by (40), flux (61) becomes

$$F_{\mathrm{CGO}}(\kappa, x) = [2\nabla S - (e^* \cdot \nabla S)e - (e \cdot \nabla S)e^*]e^{-2\kappa\phi}|A|^2 + O(1/\sqrt{\kappa}), \tag{62}$$

where the lowest order has been separated by taking into account estimate (30).

We now need the identity

$$\frac{\partial H}{\partial N_i}(x, \nabla S) = e^*(x, \nabla S) \cdot \frac{\partial \mathsf{D}_0(x, \nabla S)}{\partial N_i} e(x, \nabla S) + O(|\nabla\phi|^2),$$

which follows from the derivative of the eigenvalue equation $\mathsf{D}_0 e = He$ evaluated at $N = \nabla S$ and multiplied on the left by e^*. The $O(|\nabla\phi|^2)$ remainder stems from the fact that ∇S, with S solution to (40a), does not solve exactly the dispersion equation. One has $H(x, \nabla S) = O(|\nabla\phi|^2)$ and $e^*\mathsf{D}_0 = He^* = O(|\nabla\phi|^2)$. This holds for any choice of the remainder σ_0.

When D_0 is given by (3), cf. also Eq. (32b), the complex geometrical optics flux (62) takes the form

$$F_{\mathrm{CGO}}(\kappa, x) = V(x)e^{-2\kappa\phi(x)}|A(x)|^2 + O(1/\sqrt{\kappa}). \tag{63}$$

In physical units, the corresponding Poynting vector reads

$$\frac{c}{16\pi}F_{\mathrm{CGO}}(\kappa, x) = v_g(x)W(x) + O(1/\sqrt{\kappa}), \tag{64}$$

with v_g given by (58). In Eq. (64), however, we notice that the order of the error term is larger than the order of the difference $(V - V_\phi)e^{-2\kappa\phi}$. Therefore, Eq. (64) holds true for v_g given by (59) as well.

Concluding, both formulations give an approximation of the wave energy flux of the same order in the limit $\kappa \to +\infty$. The optimized formulation used in GRAY has the computational advantage that extended rays represent the approximated energy flow.

IV. NUMERICAL RESULTS

In this section, a few numerical tests are reported in order to illustrate the theoretical results.

First, we shall provide an estimate of the difference between the directions of the fields V and V_ϕ defined in Eqs. (44) and (45), respectively. In this case, both fields are computed by the GRAY code,[1] which employs the optimized form (46) of extended ray equations, cf. Sec. II B. With this aim, a new diagnostics has been implemented in GRAY for the calculation of the vector field V along the extended rays. We have seen in Sec. III B that the difference $V - V_\phi$ weighted with the exponential $e^{-2\kappa\phi}$ vanishes for $\kappa \to +\infty$. This formal result just means that the two vector fields are close to each other near the reference ray $\mathcal{R}$ where the field is localized. This comparison allows us to estimate their difference for realistic values of physical parameters.

Then, we shall provide a comparison between extended rays obtained by GRAY and the field lines of the vector V, as computed using the function S from the paraxial WKB code TORBEAM.[2] It is known from previous studies[9,15,32,33] that complex geometrical optics Eqs. (22) and the paraxial WKB method should give the same results within the paraxial approximation. On the other hand, GRAY solves Eqs. (46). Hence, this test provides a qualitative and quantitative estimate on the differences between the energy flows approximated by the standard and optimized forms of extended ray equations discussed in Sec. III. In addition, this numerical experiment provides a benchmark case of a new module recently added to TORBEAM, which computes the field lines of V with the aim of both representing the wave energy flow of a beam and allowing a direct coupling of TORBEAM to other ray-based codes, like quasi-linear Fokker-Planck solvers.[34] All considered cases refer to electron cyclotron beams in a standard ITER plasma equilibrium.[62]

A. Comparison of velocity fields in GRAY

The complex geometrical optics code GRAY solve Eqs. (46) with the Hamiltonian

$$H(x, N) = N^2 - n^2(x, N_\parallel),$$

where $n^2(x, N_\parallel)$ is obtained from the Altar-Appleton-Hartree dispersion relation for high-frequency waves in cold magnetized plasmas.[36] Here, $N_\parallel = b(x) \cdot N$ is the real parallel refractive index, with $b(x)$ the unit vector of the local equilibrium magnetic field. For convenience, let us introduce the imaginary part $N' = \nabla\phi$ of the refractive index.

The complex extension gives the effective Hamiltonian, cf. Eq. (23),

$$H_\phi(x,N) = N^2 - n^2(x,N_\parallel) - |\nabla\phi(x)|^2 + \frac{1}{2}\frac{\partial^2 n^2(x,N_\parallel)}{\partial N_\parallel^2}(b(x)\cdot\nabla\phi(x))^2. \quad (65)$$

At each grid point $x = (\mathrm{x},\mathrm{y},\mathrm{z})$ along extended rays, both the vector $V_\phi(x)$, tangent to the ray, and the vector $V(x)$ are evaluated. We can use the arc-length as a parametrization of the field lines of these two fields, so that only the unit vectors $v(x) = V(x)/|V(x)|$ and $v_\phi(x) = V_\phi(x)/|V_\phi(x)|$ are relevant. As an estimate of the difference, we propose the angle ϑ defined by

$$\cos\vartheta = v(x)\cdot v_\phi(x). \quad (66)$$

Figures 2–5 show the results for four cases of electron cyclotron beams, launched from the equatorial plane in

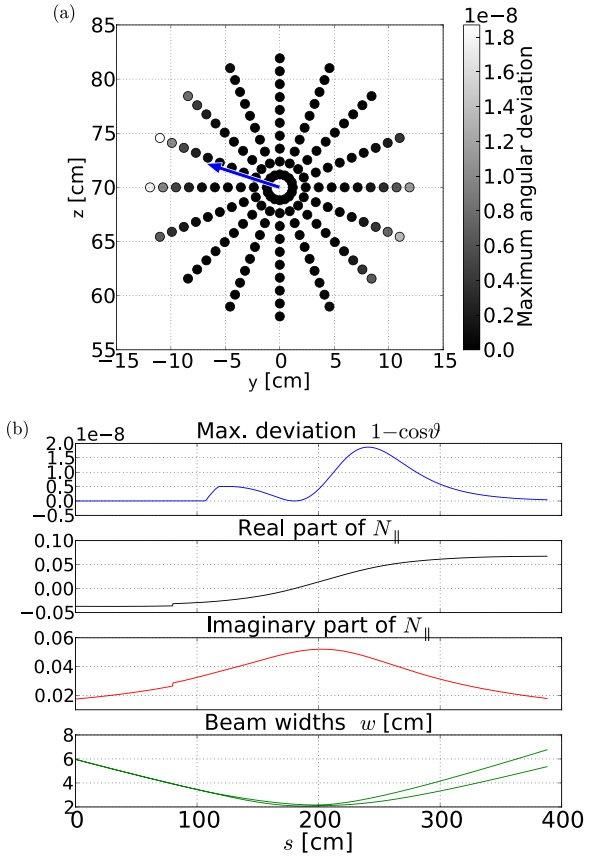

FIG. 2. Angular deviation $1-\cos\vartheta$ of extended rays, cf. Eq. (66), as computed by the GRAY code. Panel (a) shows the initial positions of extended rays, projected on the y-z plane. The gray level of each point encodes the maximum deviation observed along the corresponding ray, and the approximate direction of the equilibrium magnetic field is indicated by an arrow. Panel (b) shows the profile of the deviation for the "worst ray," compared to both the real and imaginary parts of the parallel refractive index, as well as to the two beam widths (defined as the widths of the elliptical e^{-2}-intensity contour in the beam cross-section). In this case, the equivalent focal length in free space is $z_f = 200\,\mathrm{cm}$ and the equivalent width at the waist in free space is $w_0 = 2\,\mathrm{cm}$. The poloidal and toroidal injection angles are $\alpha = 0°$ and $\beta = 0°$, respectively. The discontinuity in the parallel refractive index is due to the way the equilibrium magnetic field has been extended outside the numerical grid, in the vacuum region (we set $b = e_\phi$ outside the grid, e_ϕ being the unit vector in the toroidal direction). The Cartesian components of the refractive index are actually continuous. The initial positions of rays are given on a plane orthogonal to the injection direction, thus their projections on the x-y plane depend on the angle β.

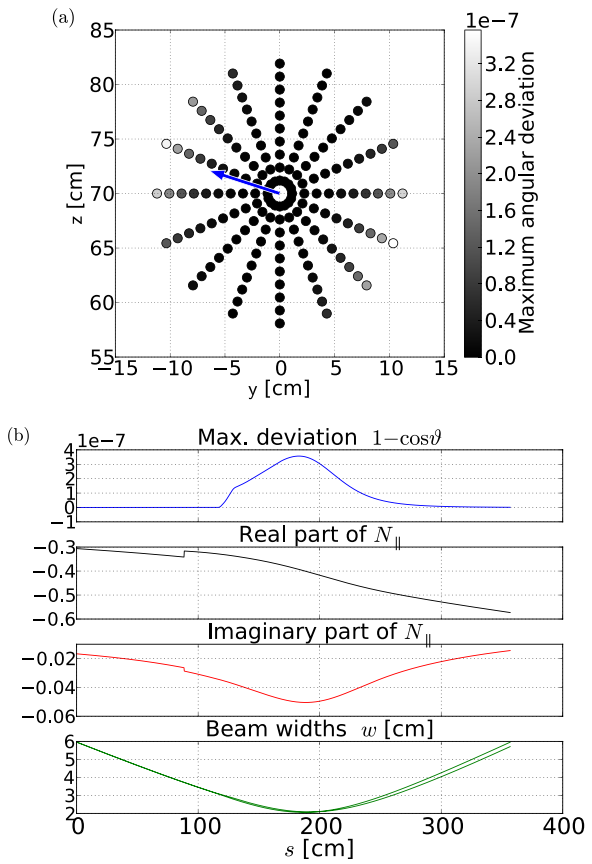

FIG. 3. The same as in Figure 2, but for $z_f = 200\,\mathrm{cm}$, $w_0 = 2\,\mathrm{cm}$, $\alpha = 0°$, and $\beta = 20°$.

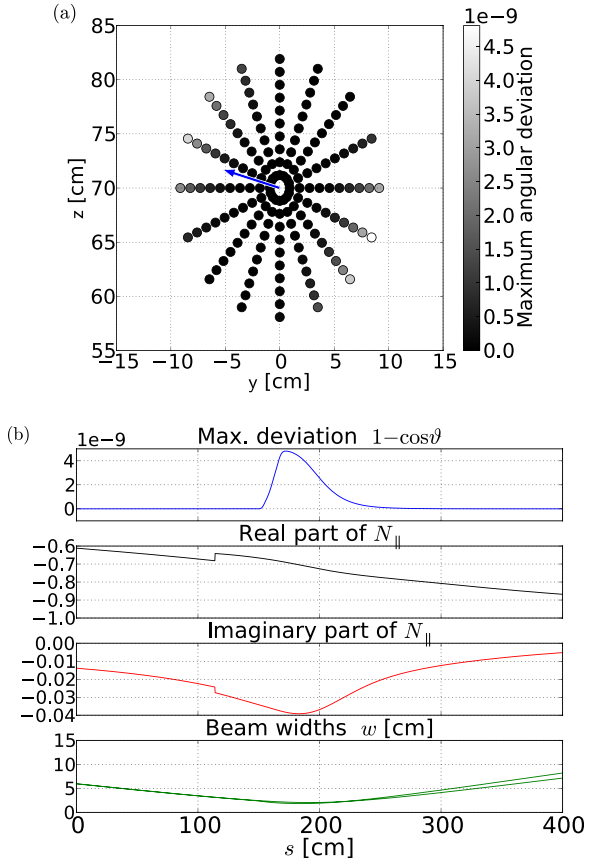

FIG. 4. The same as in Figure 2, but for $z_f = 200\,\mathrm{cm}$, $w_0 = 2\,\mathrm{cm}$, $\alpha = 0°$, and $\beta = 40°$.

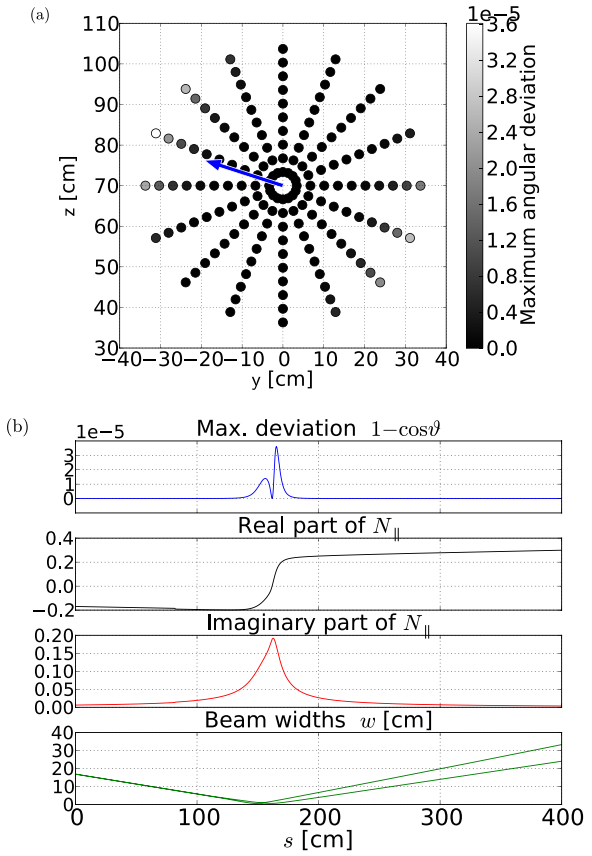

FIG. 5. The same as in Figure 2, but for $z_f = 150\,\text{cm}$, $w_0 = 0.5\,\text{cm}$, $\alpha = 0^\circ$, and $\beta = 0^\circ$.

ITER (the exact launching position of the reference ray is the same in all cases: $x = 930\,\text{cm}$, $y = 0\,\text{cm}$, and $z = 70\,\text{cm}$). In Figures 2–4, the beam has a mild focalization similar to ITER operational parameters, i.e., the equivalent focal length in free space is $z_f = 200\,\text{cm}$ with an equivalent waist $w_0 = 2\,\text{cm}$, and the beams are launched at the poloidal angle $\alpha = 0^\circ$ and different toroidal angles, namely, $\beta = 0^\circ$ (Figure 2), $\beta = 20^\circ$ (Figure 3), and $\beta = 40^\circ$ (Figure 4). In Figure 5, the results for a beam with high focalization are displayed. In this case, the equivalent focal length in free space is $z_f = 150\,\text{cm}$, with the equivalent waist $w_0 = 0.5\,\text{cm}$, poloidal injection angle $\alpha = 0^\circ$, and toroidal injection angle $\beta = 0^\circ$. Such a highly focused beam largely exceeds ITER parameters, but it has been considered as an example in which the effects of diffraction are emphasized.

Panels (a) of Figures 2–5 show the initial positions of extended rays projected in the y-z plane. One can see that rays are launched from a polar grid of points. The electric field amplitude is a Gaussian with the maximum at the center of the ray bundle (the reference ray), and points at the same radial position lie on the same amplitude level contour. For this test, a large number of rays are considered, so that the beam is covered up to the e^{-4}-level of its amplitude, a much larger beam section than usually needed. Each point is represented in a gray scale, which encodes the maximum value of the angular deviation $1 - \cos\vartheta$, with ϑ given in (66), observed along the ray issued from that point. The approximate direction of the local magnetic field in the low-field side projected onto the y-z plane is indicated by an arrow (this is approximated by the value of the numerical equilibrium magnetic field at the nearest grid node to the launching point, specifically, at major radius coordinate $R = 850.0\,\text{cm}$ and vertical coordinate $z = 70.3125\,\text{cm}$ of the numerical grid). The distribution of angular deviations allows us to appreciate geometric effects. In all considered cases, rays for which the angular deviation attains its maximum are those aligned to the magnetic field. This can be understood by inspection of the effective Hamiltonian (65). The difference between the vector fields V and V_ϕ is proportional to the product $N_\parallel (N_\parallel')^2$ of the real parallel refractive index and the square of the imaginary parallel refractive index $N_\parallel' = b(x) \cdot \nabla\phi(x)$. The factor $N_\parallel$ is obtained on noting that for the Altar-Appleton-Hartree dispersion relation, the third-order derivative of n^2, cf. Eq. (45), is proportional to $N_\parallel$, while the factor $(N_\parallel')^2$ comes from the complex extension. It follows that rays with a large $N_\parallel (N_\parallel')^2$ show larger deviations.

For each case of Figures 2–5, we have selected the "worst ray," i.e., the ray for which the maximum angular deviation is observed, and the corresponding profile of $1 - \cos\vartheta$ is plotted (panels (b)) as a function of the arc-length s along the central ray, which is used as a common parameter for all rays. The profiles of both the real and imaginary parts of the parallel refractive index, as well as the profiles of the two beam widths are also reported for a comparison. The beam widths in particular are computed according to the standard definition for Gaussian beams,[60] for which the intensity contours in the beam cross-section are ellipses. The widths are then defined as the length of the semi-axis of the e^{-2}-intensity contour.

One can see that the maximum deviation occurs, as expected, near the waist of the beam, where diffraction effects are more important, and, thus, the imaginary part of the refractive index increases. For the cases of exactly perpendicular injection (toroidal angle $\beta = 0^\circ$), a double-peak structure of the deviation profile is observed. The local minimum is found where $N_\parallel$ is zero, which implies that the difference between V and V_ϕ must vanish. In passing, let us mention that the slight discontinuity in the profiles of both the real and imaginary parallel refractive indices is due to the way the equilibrium magnetic field has been extended outside the numerical grid. There, the propagation happens in free space, and the precise value of the magnetic field is not important. We have set $b = e_\phi$ for the calculation of parallel refractive indices outside the grid, where e_ϕ is the unit vector in the toroidal direction. This choice does not match continuously to the numerical equilibrium at the boundary of the grid. The Cartesian components of the refractive index are actually continuous.

The overall conclusion from Figures 2–4 is that, under ITER-relevant conditions, the angular deviation of the two vector fields V and V_ϕ in the region of space spanned by the rays is small, i.e., of the order comparable to $\sqrt{\epsilon_{\text{mach}}}$ where ϵ_{mach} is the machine precision. Similar results are found for the highly focused beam of Figure 3, for which diffraction effects are stronger.

The good agreement of velocity fields as computed by GRAY confirms the theoretical estimate of the difference (60) for finite values of κ. This result alone however does

not allow us to draw any conclusion on the approximation of the energy flow. In fact, the GRAY code uses the optimized form (46) of extended ray equations, hence the vector V computed here does not correspond exactly to the energy flow computed according to (58). Moreover, the integral lines of two vector fields might exhibit differences even when the vector fields themselves are very similar.

In Sec. IV B, we shall give a more quantitative estimate of the difference between the approximations of the wave energy flow.

B. Extended rays versus paraxial WKB energy flux

Equation (40a), Taylor-expanded around the curve $\mathcal{R}$, yields the matrix Riccati equation for the Hessian of the phase of the paraxial WKB method.[9] This shows that the paraxial WKB solution for both the real part $S(x)$ and the imaginary part $\phi(x)$ of the complex eikonal is a good approximation of the corresponding quantities computed directly via the standard extended ray Eqs. (22). This argument is referred to as Gaussian limit of complex geometrical optics.[32,33] In this limit, the paraxial WKB calculation of flow of V yields a good approximation of the energy flow obtained in the standard extended ray theory from the group velocity (58). On the other hand, the GRAY code solves the optimized form (46). Extended rays thus obtained represent the energy flow corresponding to the group velocity (59). We shall now compare those two equivalent approximations of the wave energy flow.

This is made possible by a recently added module[34] of the paraxial WKB code TORBEAM, which computes the field lines of V. Specifically, the new module solves the set of ordinary differential equations

$$\frac{dx}{d\tau} = V(x), \tag{67}$$

where $V(x)$ is defined by (44), with the real phase S being here computed in the paraxial WKB framework. The result is a bundle of curves that represents the energy flow of the beam in the paraxial WKB method.

Figure 6 shows a qualitative comparison between the extended rays computed by GRAY and the TORBEAM solution of Eq. (67) with initial conditions given by the initial position of GRAY rays. We refer to the latter as TORBEAM rays, for simplicity. The case considered is the same as that of Figure 2, with focusing typical for ITER parameters. The projections of both GRAY and TORBEAM rays into the x-z poloidal plane (a) and into the y-z plane (b) are shown for the rays corresponding to the e^{-2}-level of the amplitude only. The common initial positions of rays are marked by dots. In the poloidal projection (a), one should notice the rather long propagation of the beam. The x-axis scale is very different from that of the z-axis. Nonetheless, the two set of rays follow each other precisely up to the waist of the beam, where diffraction effects are stronger. At the waist, the differences between the flows start to be significant. Even after a long propagation length however, the cumulative effects of such differences are much smaller than the beam width.

This comparison has been repeated for the highly focused case of Figure 5, and the results are displayed in Figure 7. The behavior is the same as in Figure 6, but here the beam width is one order of magnitude larger, while the beam waist is much smaller due to the strong focusing. Diffraction effects are stronger and result in larger deviations of the two set of rays near the waist. Nonetheless, the deviations of the rays are still smaller than the beam width.

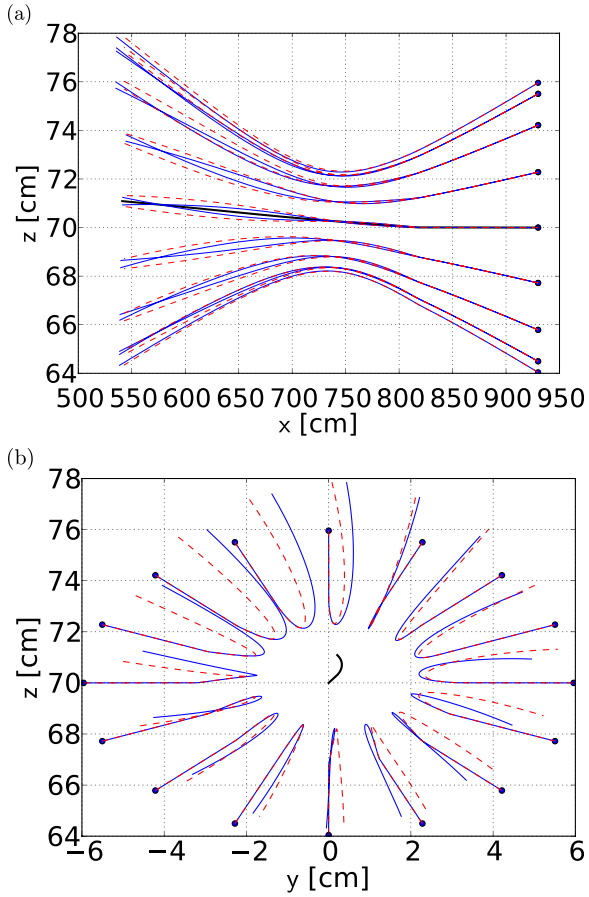

FIG. 6. Visualization of extended rays for the case $z_f = 200\,\text{cm}$, $w_0 = 2\,\text{cm}$, and $\alpha = \beta = 0°$ of Figure 2. The projection of rays on the x-z plane (a) and on the y-z plane (b) shows the differences between GRAY rays (dashed, red, curves) and TORBEAM rays (solid, blue, curves). The central ray is also shown (thick, black, curve) at the center of the beam.

Quantitatively, we can compute the distance of the positions of GRAY and TORBEAM rays issued from the same point at a given value of the arc-length s. For the mildly focused case of Figure 6, we choose $s = 380\,\text{cm}$ and we find that the distance in the worst case is 0.86 cm. Similarly, for the highly focused case of Figure 7, we choose $s = 390\,\text{cm}$ and we find a distance of 6.91 cm. The three-dimensional trajectories of the corresponding pair of rays are shown in Figure 8. The distances should be compared with the beam width, which is $\approx$6 cm for the case of Figure 8(a) and $\approx$30 cm for the case of Figure 8(b). Deviations are, therefore, 14.4% and 23.0% of the beam width, respectively.

The beam width is the natural reference parameter against which the distances are compared. One should notice however that those numbers refer to the worst pair of rays, and the three-dimensional positions do not lie on the same beam cross section. Therefore, these results tend to overestimate the difference between the two approximated energy flows.

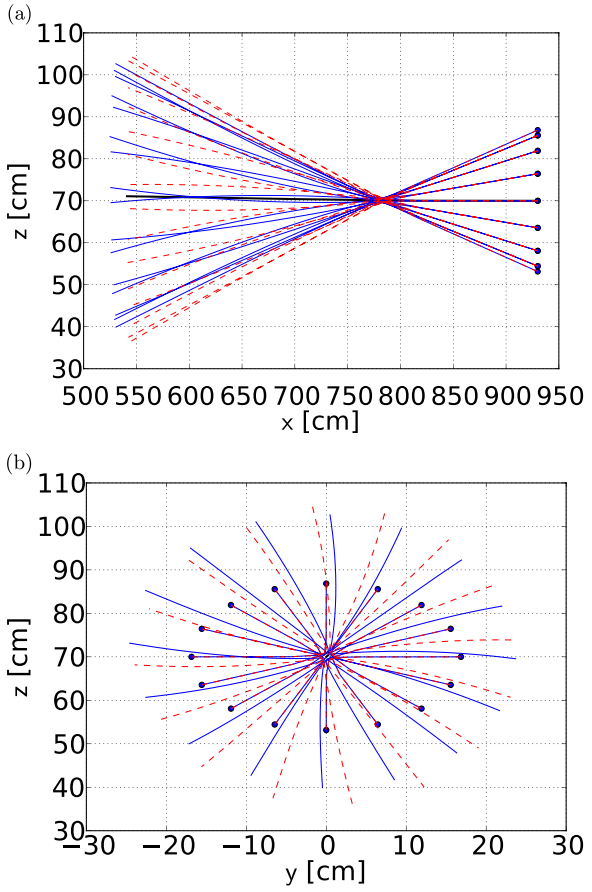

FIG. 7. The same as in Figure 6, but for the highly focused case, $z_f = 150\,\text{cm}$, $w_0 = 0.5\text{cm}$, and $\alpha = \beta = 0°$ of Figure 5.

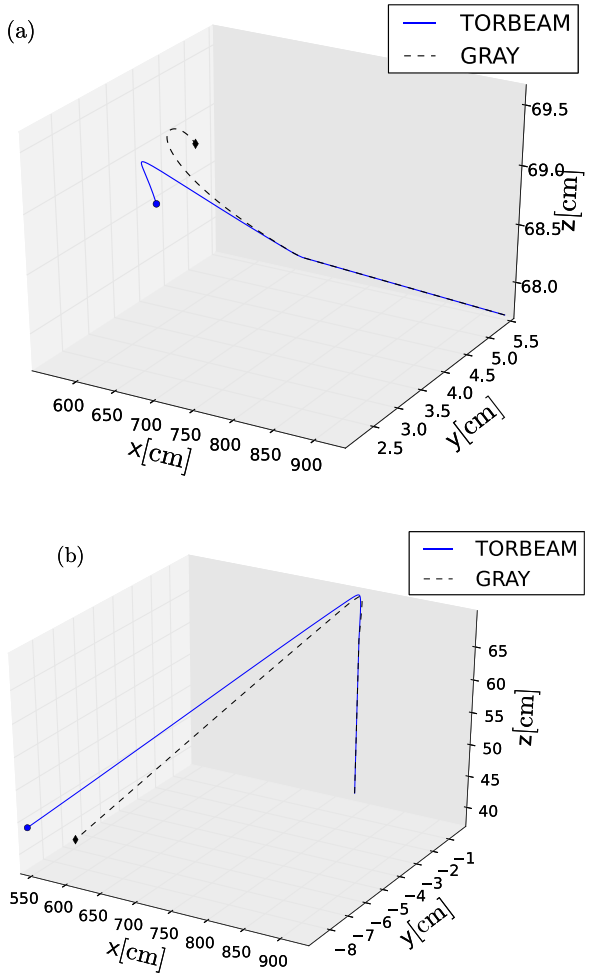

FIG. 8. Three-dimensional trajectories of the pair of GRAY and TORBEAM rays with the largest difference in position after a fixed arc-length s. Plot (a) shows the results for the case of Figure 6, with $s = 380\text{cm}$. The positions reached after the prescribed arc-length are marked on both rays and correspond to coordinates (in cm) $(550.06, 4.27, 68.48)$ for the TORBEAM ray and $(550.07, 5.07, 68.79)$ for the GRAY ray, at the distance of 0.86cm. Plot (b) is for the case of Figure 7 with $s = 390\text{cm}$. The reached positions correspond to the coordinates $(542.48, -8.97, 44.06)$ for the TORBEAM ray and $(543.16, -6.65, 37.58)$ for the GRAY ray, at the distance of 6.91cm.

The foregoing results give an estimate of the difference between the two independent approximations of the wave energy flux obtained from the standard and optimized formulations of extended ray theory, cf. Sec. III B.

In addition, this comparison illustrates how the information on extended rays is actually encoded in the paraxial WKB solution as well, despite the fact that the paraxial approach describes the wave beam through a set of parameters on a single ray, namely, the reference ray.

V. ACCOUNTING FOR SPATIAL DISPERSION

The theory reported in Sec. III is by no means limited to the case of Eq. (1). In this section, we show how the generic case of a spatially dispersive media can be addressed. We shall see that this approach is actually more general and applies to a wide range of high frequency wave propagation problems.

Let us start recalling the definition of spatially dispersive media. In Eq. (1), the electric displacement D is related to the electric field E through the constitutive relationship $D(\kappa, x) = \varepsilon(\kappa, x)E(\kappa, x)$. This is a local relation in the sense that both D and E are evaluated at the same point x. The cold plasma model[36] is an example of a system with a local constitutive relationship. In general, however, the plasma response to an electromagnetic disturbance is more complicated as non-local effects can set in. The electric displacement $D(\kappa, x)$ in a point x depends on the electric field $E(\kappa, x')$ in a different point x' through an integral operator, which can be written in the pseudodifferential form[6]

$$D(\kappa, x) = \left(\frac{\kappa}{2\pi}\right)^d \int e^{i\kappa(x-x')\cdot N} \varepsilon\left(\kappa, \frac{1}{2}(x+x'), N\right) E(\kappa, x') dx' dN, \tag{68}$$

where $\varepsilon(\kappa, x, N)$ is the dielectric tensor, depending now on the refractive index N. A medium with such a response is referred to as a spatially dispersive medium, because the dielectric tensor is different for waves with different wave vectors. The results of Sec. III generalize to spatially dispersive media as far as condition (2) is fulfilled for $\varepsilon(\kappa, x, N)$. In particular, the leading order $\varepsilon_0(x, N)$ should be Hermitian.

For electron cyclotron beams in tokamak physics, spatial dispersion is found as a consequence of temperature effects in the response of the plasma[35] and might be a concern for high temperature devices. For present day machines, temperature effects are neglected up to the region where the beam is

absorbed by resonating electrons. There, the non-local response and thus spatial dispersion must be dealt with, but in such situation condition (2) is violated, thus turning our dispersive generalization of complex geometrical optics into a mere theoretical exercise. Nonetheless, from the point of view of the theory of the complex geometrical optics, the issue of the generalization is interesting. We give here a sketch of the derivation only.

The basic idea is to take advantage of the pseudodifferential form the wave equation for a generic dispersive stationary medium.[6] With the constitutive relation (68), Maxwell's equations amount to

$$\mathsf{D}^w\left(\kappa,x,-\frac{i}{\kappa}\nabla\right)E(\kappa,x)=\left(\frac{\kappa}{2\pi}\right)^d\int e^{i\kappa(x-x')\cdot N}\times\mathsf{D}\left(\kappa,\frac{1}{2}(x+x'),N\right)E(\kappa,x')dx'dN=0, \tag{69}$$

where

$$\mathsf{D}_{ij}(\kappa,x,N)=N^2\delta_{ij}-N_iN_j-\varepsilon_{ij}(\kappa,x,N)$$

is the Weyl symbol[6,37] of the semiclassical pseudodifferential operator $\mathsf{D}^w(\kappa,x,-(i/\kappa)\nabla)$, $1/\kappa$ being the semiclassical parameter.

Assuming the equivalent of condition (2), one has

$$\mathsf{D}(\kappa,x,N)=\mathsf{D}_0(x,N)+\frac{1}{\kappa}\mathsf{D}_1(x,N)+\cdots,$$

where the leading order term (i.e., the semiclassical principal symbol[37]) is Hermitian. Like in the non-dispersive case, we assume that the (real) eigenvalues of D_0 are well separated, as discussed in Sec. II A, so that we do not have to worry about linear mode conversion.

Let us start deriving a useful asymptotic form of the wave equation. We consider the electric field in the form

$$E(\kappa,x)=e^{i\kappa S(x)}w(\kappa,x), \tag{70a}$$

where the amplitude $w(\kappa,x)$ is allowed to have fast variations, namely,

$$|\partial_x^\alpha w(\kappa,x)|\le C\kappa^{r|\alpha|}, \tag{70b}$$

where C is a constant depending only on the multi-index $\alpha=(\alpha_1,\ldots,\alpha_d)$, and r is a fixed real parameter with $0\le r<1$. Each derivative increases the order by a factor κ^r. The fast variations of the amplitude distinguish the wave field (70) from the standard (real) eikonal wave (4).

The complex eikonal wave (25) has the form (70), with

$$w(\kappa,x)=e^{-\kappa\phi(x)}a(\kappa,x), \tag{71}$$

and $r=1/2$, provided that the two conditions on the paraxial field, cf. Sec. II C, are fulfilled. This follows from estimate (30), which allows us to control the derivative,

$$|\nabla(e^{-\kappa\phi(x)}a(\kappa,x))|\le C_0+\kappa C_1|\nabla\phi e^{-\kappa\phi(x)}a(\kappa,x)|=O(\sqrt{\kappa}).$$

The substitution of the field (70) into the wave Eq. (69), along with lengthy but standard calculations,[6] yields

$$\frac{i}{\kappa}\frac{\partial\mathsf{D}_0}{\partial N_k}\frac{\partial w}{\partial x^k}+\frac{1}{2\kappa^2}\frac{\partial^2\mathsf{D}_0}{\partial N_k\partial N_l}\frac{\partial^2 w}{\partial x^k\partial x^l}-\left[\mathsf{D}_0-\frac{i}{2\kappa}\left(\frac{\partial}{\partial x^k}\left[\frac{\partial\mathsf{D}_0}{\partial N_k}\right]+2i\mathsf{D}_1\right)\right]w+O(\kappa^{-3/2})=0, \tag{72}$$

where the case $r=1/2$ has been considered. One can now substitute the form (71) specific to complex eikonal waves, with the amplitude given by (25b) and, collecting terms, one has

$$e^{i\kappa\psi}\left\{\tilde{\mathsf{D}}_0(x,\nabla\psi)a_0(x)+\frac{1}{\kappa}\left[\mathsf{D}_0(x,\nabla S)a_1-i\left[\frac{\partial\mathsf{D}_0}{\partial N_i}(x,\nabla S)\frac{\partial a_0}{\partial x^i}+\frac{1}{2}\left[\frac{\partial^2\mathsf{D}_0}{\partial x^i\partial N_i}(x,\nabla S)+\frac{\partial^2\psi}{\partial x^i\partial x^j}\frac{\partial^2\mathsf{D}_0}{\partial N_i\partial N_j}(x,\nabla S)\right]a_0+i\mathsf{D}_1a_0\right]\right]\right\}+O(\kappa^{-3/2})=0, \tag{73}$$

where $\psi=S+i\phi$ and

$$\tilde{\mathsf{D}}_0(x,\tilde{N})=\mathsf{D}_0(x,N)+i\frac{\partial\mathsf{D}_0(x,N)}{\partial N_k}N_k'-\frac{1}{2}\frac{\partial^2\mathsf{D}_0}{\partial N_k\partial N_l}N_k'N_l'.$$

Equation (73) (except for an overall factor κ^2) is formally the same as Eq. (34), with the only difference that the complex extension $\tilde{\mathsf{D}}_0$ needs to be considered, with the dispersion tensor D_0 given by the principal part of the Weyl symbol in (69). In addition, $-\varepsilon_1$ is replaced by D_1. Particularly, the complex extension $\tilde{\mathsf{D}}_0$ is found here naturally in the very same form as that used in the solution of Eq. (35a) of Sec. III.

With such replacements being implied, we can conclude that the results on the complex geometrical optics solution are also valid for dispersive media. Let us also remark that this approach does not take advantage of the specific form of the symbol $\mathsf{D}(\kappa,x,N)$. The results are, therefore, valid for a broader class of wave equations, i.e., semiclassical pseudodifferential wave equations having a sufficiently regular symbol with a Hermitian principal part.

VI. CONCLUSIONS

A systematic derivation of the equations of extended ray tracing with improved error control has been presented. The main element of novelty in this derivation consists in the use of two simple but crucial inequalities introduced by Pereverzev[9] and Maslov[10] independently in different contexts.

With respect to the standard derivation, which relies on formal Taylor expansions, such inequalities yield a sharper control of the order of terms in the asymptotic expansion of the wave equation in the high frequency limit.

The leading order term in the asymptotic expansion is found to be defined apart from an arbitrary remainder. When that is set to zero, we recover the standard equations of extended ray tracing already known in literature.[28–33]

Alternatively, the choice of the arbitrary remainder allows us to improve the geometric properties of extended rays, obtaining the form of extended ray equations implemented in the GRAY[1] code.

At the next order, the equation for the transport of the complex amplitude is obtained. Here, the advantages of the sharper error control are manifest. The transport equation is obtained in a much simpler form, from which the wave energy flux vector can be readily identified. This is the main physics result of the paper.

The theory is illustrated by a number of numerical experiments performed with the GRAY[1] and TORBEAM[2] codes, for electron cyclotron beams in tokamak plasmas. The numerical results allow us to quantify the effects of the choice of the arbitrary remainders on the approximation of the wave energy flux vector and of the corresponding energy flow.

ACKNOWLEDGMENTS

Many ideas, upon which we have strongly relied in developing our arguments, are Grigory Pereverzev's. His keen insights and guidance are deeply missed.

O.M. wish to thank Marino Bornatici and Roberto Pozzoli for many discussions, constructive criticisms, and tutorship during his Ph.D. work, which in part has been used here. A.M. wish to thank Roberto Pozzoli for the tutorship during his Master degree and Ph.D. work on this subject and Lorenzo Figini for the help with the GRAY code.

We are grateful to the anonymous referee for his/her careful reading, many suggestions and interesting insights that contributed significantly to improve the paper in both form and content.

[1]D. Farina, Fusion Sci. Technol. **52**, 154 (2007).
[2]E. Poli, A. G. Peeters, and G. V. Pereverzev, Comput. Phys. Commun. **136**, 90 (2001).
[3]R. Prater, D. Farina, Yu. Gribov, R. W. Harvey, A. K. Ram, Y.-R. Lin-Liu, E. Poli, A. P. Smirnov, F. Volpe, E. Westerhof, A. Zvonkov, and ITPA Steady State Operation Topical Group, Nucl. Fusion **48**, 035006 (2008).
[4]V. M. Babič and V. S. Buldyrev, *Short-Wavelength Diffraction Theory* (Springer-Verlag, Berlin, 1991.
[5]Yu. A. Kravtsov and Yu. I. Orlov, *Geometrical Optics of Inhomogeneous Media* (Springer, Berlin, 1990).
[6]S. W. McDonald, Phys. Rep. **158**, 337–416 (1988).
[7]J. Rauch, *Lectures on Geometric Optics*, IAS-Park City Math. Ser. 5 (AMS. Providence, RI, 1998).
[8]G. V. Pereverzev, in *Reviews of Plasma Physics*, edited by B. B. Kadomtsev (Consultants Bureau, New York, 1996), Vol. 19.
[9]G. V. Pereverzev, Phys. Plasmas **5**, 3529 (1998).
[10]V. P. Maslov, *The Complex WKB Method for Nonlinear Equations I: Linear Theory* (Birkhäuser, Basel, 1994).
[11]M. M. Popov, *Ray Theory and Gaussian Beam Method for Geophysicists* (EDUFBA, Salvador-Bahia, 2002).
[12]M. Motamed and O. Runborg, Wave Motion **47**, 421 (2010).
[13]G. Ariel, B. Engquist, N. M. Tanushev, and R. Tsai, J. Comput. Phys. **230**, 2303 (2011).
[14]E. Heyman and L. B. Felsen, J. Opt. Soc. Am. A **18**, 1588 (2001).
[15]M. Bornatici and O. Maj, Plasma Phys. Controlled Fusion **45**, 707 (2003).
[16]Yu. A. Kravtsov and P. Berczynski, Stud. Geophys. Geod. **51**, 1 (2007).
[17]Yu. A. Kravtsov, *Geometrical Optics in Engineering Physics* (Alpha Science, Harrow, UK, 2005).
[18]V. Černevý, *Seismic Ray Theory* (Cambridge University Press, Cambridge, 2001).
[19]Yu. A. Kravtsov, G. W. Forbes, and A. A. Asatryan, *in Progress in Optics*, edited by E. Wolf (Elsevier, Amsterdam, 1999), Vol. XXXIX, pp. 1–62.
[20]C. J. Thomson, Stud. Geophys. Geod. **41**, 345 (1997).
[21]S. J. Chapman, J. M. H. Lawry, J. R. Ockendon, and R. H. Tew, SIAM Rev. **41**, 417 (1999).
[22]R. A. Egorchenkov and Yu. A. Kravtsov, J. Opt. Soc. Am. A **18**, 650 (2001).
[23]D. Amodei, H. Keers, D. Vasco, and L. Johnson, Phys. Rev. E **73**, 036704 (2006).
[24]A. Bravo-Ortega and A. H. Glasser, Phys. Fluids B **3**, 529 (1991).
[25]A. Cardinali, in *Proceedings of the 14th International Conference on Radio Frequency Power in Plasmas* (Oxnard, California, 2001), p. 166.
[26]A. Cardinali, "Theory of Fusion Plasmas," in *Proceedings of the International School of Plasma Physics "Piero Caldirola," Varenna, Italy* (2000), p. 439.
[27]S. Choudhary and L. B. Felsen, IEEE Trans. Antennas Propag. **21**, 827 (1973).
[28]E. Mazzucato, Phys. Fluids B **1**, 1855 (1989).
[29]S. Nowak and A. Orefice, Phys. Fluids B **5**, 1945 (1993).
[30]S. Nowak and A. Orefice, Phys. Plasmas **1**, 1242 (1994).
[31]S. Nowak and A. Orefice, J. Plasma Phys. **57**, 349 (1997).
[32]A. G. Peeters, Phys. Plasmas **3**, 4386 (1996).
[33]A. V. Timofeev, Phys. Usp. **48**, 609 (2005).
[34]O. Maj, E. Poli, and E. Westerhof, J. Phys.: Conf. Ser. **401**, 012013 (2012).
[35]M. Bornatici, R. Cano, O. De Barbieri, and F. Engelmann, Nucl. Fusion **23**, 1153 (1983).
[36]D. B. Melrose and R. C. McPhedran, *Electromagnetic Processes in Dispersive Media* (Cambridge University Press, Cambridge, 1991).
[37]A. Martinéz, *An Introduction to Semiclassical and Microlocal Analysis* (Springer-Verlag, New York, 2002).
[38]R. G. Littlejohn and W. G. Flynn, Phys. Rev. A **44**, 5239 (1991).
[39]L. Friedland and A. N. Kaufman, Phys. Fluids **30**, 3050 (1987).
[40]E. R. Tracy and A. N. Kaufman, Phys. Rev. E **48**, 2196 (1993).
[41]E. R. Tracy, A. N. Kaufman, and A. J. Brizard, Phys. Plasmas **10**, 2147 (2003).
[42]A. Jaun, E. R. Tracy, and A. N. Kaufman, Plasma Phys. Controlled Fusion **49**, 43 (2007).
[43]C. Emmrich and A. Weinstein, Commun. Math. Phys. **176**, 701 (1996).
[44]A. N. Kaufman, H. Ye, and Y. Hui, Phys. Lett. A **120**, 327 (1987).
[45]J.-D. Benamou, J. Sci. Comput. **19**, 63 (2003).
[46]J.-D. Benamou, O. Lafitte, R. Sentis, and I. Solliec, J. Comput. Appl. Math. **156**, 93 (2003).
[47]J.-D. Benamou, O. Lafitte, I. Solliec, and R. Sentis, J. Comput. Appl. Math. **167**, 91 (2004).
[48]O. Runborg, Commun. Comput. Phys. **2**, 827 (2007).
[49]M. E. Taylor, *Partial Differential Equations I: Basic Theory*, 2nd edition (Springer, New York, 2011).
[50]V. P. Maslov and M. V. Fedoriuk, *Semi-Classical Approximation in Quantum Mechanics* (D. Reidel Pub. Co., Dordrecht, Holland, 1981) (in Russian).
[51]L. Hörmander, *The Analysis of Linear Partial Differential Operators I* (Springer, Berlin, 1983). Sec. 6.4.
[52]J. J. Duistermaat, *Fourier Integral Operators*, Progress in mathematics (Birkhäuser, Boston, 1996).
[53]V. Guillemin and S. Sternberg, *Geometric Asymptotics*, Mathematical Surveys N. 14 (AMS, Providence, 1977).
[54]E. R. Tracy, A. J. Brizard, D. Johnston, A. N. Kaufman, A. S. Richardson, and N. Zobin, Commun. Nonlinear Sci. Numer. Simul. **17**, 2161 (2012).
[55]L. Hörmander, *Lectures on Nonlinear Hyperbolic Differential Equations* (Springer, Berlin, 1997).
[56]J. F. Nye, *Natural Focusing and the Fine Structure of Light* (IoP Publishing, Bristol, 1999).
[57]Yu. A. Kravtsov and Yu. I. Orlov, Sov. Phys. Usp. **23**, 750 (1980).
[58]O. Maj, "Complex geometric optics for symmetric hyperbolic systems I: Linear theory," e-print arXiv:0802.1691v1 [math-ph], section 3.
[59]M. Born and E. Wolf, *Principles of Optics* (Pergamon, Oxford, 1980), pp. 447–448.
[60]E. Poli, G. V. Pereverzev, A. G. Peeters, and M. Bornatici, Fusion Eng. Des. **53**, 9 (2001).
[61]J. D. Jackson, *Classical Electrodynamics*, 3rd ed. (John Wiley and Sons, Inc., New York, 1999), Sec. 6.9.
[62]G. Ramponi, D. Farina, M. A. Henderson, E. Poli, O. Sauter, G. Saibene, H. Zohm, and C. Zucca, Nucl. Fusion **48**, 054012 (2008).